Resonance frequency and stability of composite micro/nanoshell via deep neural network trained by adaptive momentum-based approach

Yunrui Yan*

College of Material science and Nanoengineering, Rice University, Houston 77005, Texas, USA

Abstract.   In the present study, the effects of thermal loading on the buckling and resonance frequency of graphene platelets (GPL) reinforced nano-composites are examined. Functionally graded (FG) material properties are considered in thickness direction for the thermal responses of the composite. The equivalent material properties are obtained using Halphin-Tsai nano-mechanical model for composite layers. Moreover, the effects of nano-scale sizes are taken into account, employing functionally modified couple stress (FMCS) parameter. In this regard, for the first time, it is demonstrated that at certain values of GPL weight fraction, thermal buckling occurs. In obtaining results of vibrational behavior, both analytical solution and deep neural network (DNN) methods are used. The DNN method needs low computational costs to predict the resonance behavior. A comprehensive parametric study is conducted to indicate the effects of several geometrical, material, and loading conditions on the vibrational and buckling behavior of cylindrical shell structures made of GPL-nanocomposites. It is shown that the effect of temperature change on the occurrence of buckling is vital while it has a negligible impact on the resonance frequency of the structure. Moreover, the size-dependency of the results is demonstrated, and it cannot be neglected in nano-scales.

Keywords: graphene nano-platelet; modified couple stress parameter; resonance frequency; thermal buckling; various thermal distributions

1. Introduction

GPL reinforced nanocomposites have been shown to demonstrate exceptional properties under mechanical, electrical, and thermal loads. Ref (Habibi *et al.* 2016, Habibi *et al.* 2018, Ebrahimi *et al.* 2019a, Esmailpoor Hajilak *et al.* 2019, Ghabussi *et al.* 2019, Safarpour *et al.* 2020, Shariati *et al.* 2020a) listed applications reported in the literature for these nanostructure materials. Due to such properties in GPL-reinforced composites, they become a proper candidate in nano-engineering, chemistry, electrical and physics applications (Shi *et al.* 2018). Investigation of material properties and responses under various loadings is important to have a broader understanding of such materials (Zhang *et al.* 2016, Ni *et al.* 2020a, Ni *et al.* 2020b, Ding *et al.* 2021, Meng *et al.* 2021, Yu *et al.* 2021). Size-dependency in nano-structure materials is an important issue that cannot be reflected in the classical theories of continuum mechanics. Thus, several size-dependent theories have been proposed to incorporate the effect of nano and microscale in the analyses. One of the most effective theories in this field is the couple stress theory. Khorasani *et al.* (2020) investigated the vibrational behavior of 3-layer composite material under several multiphysics loads using the modified couple stress theory. In their analysis, they found the considerable effects of length scale on the natural frequencies of the structure. Alimirzaei *et al.*

(2019) investigated vibrational, buckling, and bending responses of beams in microscale using finite element method. Effects of various loading condition on natural frequencies of micro-beam was comprehensively reported in their study. Tlidji *et al.* (2019) examined the influence of different indices of functionally graded material on the frequency response of beams in a micro-scale. They employed modified coupled stress to observe the effects of size on the response of the beam. One of the theories incorporating short length of beams is first-order shear deformation theory (FSDT) which is extensively used in the analysis of structures on a micro-scale. Bourada *et al.* (2020) used FSDT to derive equations of motion of a composite beam resting on an elastic foundation. In their analyses, they reported the effects of various geometrical and material parameters on the vibrational stability of the beam. Matouk *et al.* (2020) employed the nonlocal theory of Eringen to investigate the vibration of microbeam in thermal and moisture environments. A discussion of the effects of size and different material and geometrical parameters was also presented. Matuk *et al.* (Bousahla Abdelmoumen *et al.* 2020) employed FSDT to investigate buckling and frequency responses of single-walled carbon nanotube composite beams on an elastic substrate. They presented effects of various parameters on the static and dynamic stability of the structure. Draiche *et al.* (2019) utilized simple FSDT formulation to analyze the vibrational behavior of composite plates under simple boundary conditions. Shells structure, due to their complicated equations of motion, also attracted much attention in the literature. Allam *et al.* (2020) used refined higher-order shear deformation theory to analyze static and vibrational

---

*Corresponding author.
E-mail: yy92@rice.edu

Table 1 First three natural frequencies obtained from this study in comparison to the results of Ref (Tadi Beni *et al.* 2016) for isotropic homogeneous nanoshells, with different thicknesses, L/R=10 and m=1

h	Mode number	Ref (Tadi Beni *et al.* 2016) (CT)	Current study (CT)	Ref (Tadi Beni *et al.* 2016) (MCST)	Current study (MCST)
	1	0.1954	0.19536215	0.1955	0.19543206
0.02R	2	0.2532	0.25271274	0.2575	0.25731258
	3	0.2772	0.27580092	0.3067	0.30621690
	1	0.1959	0.19542305	0.1963	0.19585782
0.05R	2	0.2623	0.25884786	0.2869	0.28543902
	3	0.3220	0.31407326	0.4586	0.45457555

Table 2 Predicted results obtained from trained DNN using various values of MSN g_{GPL} and l/R parameters

g_{GPL} (%)	Fit	Predicted		
		$MSE_{Train} = 0.22 \times 10^{-6}$	$MSE_{Train} = 0.31 \times 10^{-6}$	$MSE_{Train} = 0.35 \times 10^{-6}$
l/R=0				
0.1	0.450	0.401	0.441	0.448
0.15	0.472	0.453	0.476	0.473
0.2	0.493	0.552	0.498	0.494
l/R=0.1				
0.1	0.596	0.564	0.590	0.595
0.15	0.625	0.632	0.628	0.626
0.2	0.644	0.601	0.639	0.641
l/R=0.2				
0.1	0.729	0.767	0.735	0.731
0.15	0.745	0.700	0.739	0.743
0.2	0.772	0.712	0.765	0.769

responses of laminated composite shells. They obtained displacement and stress fields in these structures in the static analysis section. Moreover, the free vibration behavior of the shell structure is examined and compared to the results of other shear deformation theories. Hussain *et al.* (2020) investigated functionally graded shells to obtain their natural frequencies under various boundary conditions. The influence of various geometrical parameters, including height to radius ratio and length to radius ratio, on the vibrational behavior of the structure, were considered. Asghar *et al.* (2020) studied wave propagation characteristics in zigzag and chiral double-walled carbon nanotubes (DWCNTs). In their stydies, they utilized Eringen's nonlocal elasticity theory along with Donnell shell theory to obtain the effects of geometry on the vibration of DWCNTs. In a similar study, Hussain *et al.* (2019) considered the vibrational behavior of single-walled carbon nanotubes (SWCNTs) using nonlocal elasticity theory. Nonlocal strain gradient theory was coupled with higher-order shear deformation theories to obtain wave propagation patterns in functionally graded nanoshells in a study by Karami *et al.* (2019). They considered effects of

initial stresses in their analytical solutions. The working conditions of the GPL-nanocomposites are very diverse. In many circumstances, these structures are exposed to thermal environments. Thermal load applied to these composites significantly alters their vibrational and buckling properties. Rafrafi *et al.* (2020) investigated buckling behavior of sandwich plates under hygrothermal loadings. They examined effects of several parameters including moisture concentration on the buckling of functionally graded plates on elastic foundation. In a similar study, Tounsi *et al.* (2020) explored the effects of mechanical and hygro-thermal loading on the stress and displacement fields of functionally graded ceramic-metal plates. A discussion on the influence of loading and surrounding conditions was presented in their research work. Nonlinear thermal loading effects on the flexural responses of anti-symmetric plated was the subject of a study by Belbachir *et al.* (2020). A higher-order shear deformation theory was employed to analyze the thermo-mechanical loading effects on the bending behavior of FG plates in the research study by Boussoula *et al.* (2020a, b). They used a simplified n-th order shear deformation theory in the investigation of reinforcement

volume fraction effects on the static response of the structure. A novel four variable plate theory was introduced by Abualnour *et al.* (2019) to obtain displacement field in anti-symmetric composite plates. Moreover, effects of nonlinear coupled thermal and mechanical loading conditions on the bending characteristics of laminated plates were studied by Belbachir *et al.* (2019). There are many other studies in the field of thermal loading and thermal environment influences on the bending and vibrational analyses of composite plates and shells which indicates the importance of these loading conditions on the behavior of such structures (Habibi *et al.* 2019a, Safarpour *et al.* 2019a, Al-Furjan *et al.* 2020a, Alipour *et al.* 2020, Ebrahimi *et al.* 2020a, Ghabussi *et al.* 2020). Recent studies on the stability investigation of nano-composites are focused on the novel reinforcements effects and loading conditions (Habibi *et al.* 2018, Habibi *et al.* 2019b, Habibi *et al.* 2019c, Habibi *et al.* 2019d, Pourjabari *et al.* 2019, Safarpour *et al.* 2019b; Moayedi *et al.* 2020a; Shokrgozar *et al.* 2020a). Menasria *et al.* (2020) considered effects of different boundary conditions on the dynamic stability of FG plates using a novel approach to obtain governing equations. Refined shear deformation theory was employed to examine the effects of porosity on the displacement and stress fields of FG plates by Zine *et al.* (2020). A comparison of different theories incorporating size effects was implemented in the work of Domenico *et al.* (2018), along with the utilization of a novel model. They examined the wave propagation in carbon nanotubes regarded as beam structures. The results of the new theory were further compared with the results of molecular dynamics. In another study, Domenico *et al.* (2019) introduced a three-length-scale gradient elasticity theory to capture dispersive nature of wave propagation in nano-scale composite materials. A comparison of the results of the new theory with experimental results were also presented. Another novel elasticity model to investigate wave propagation in micro-scale beams coupling inertia gradient, strain gradient, and surface energy was proposed by Zhang *et al.* (2020). It was revealed that using this novel theory, the mode shapes of the beam under consideration were different from classical mode shapes. Challamel *et al.* (2018) investigated static and dynamic behaviors of nano-rod in an elastic medium. They showed that the nonlocal elasticity solution could follow lattice mechanic results accurately. To the best of author's knowledge, the effect of the thermal environment on the buckling and excitation of cylindrical shells is not reported in the literature. Therefore, in the present study, the effects of thermal loadings on the buckling and resonance frequency of graphene reinforced nano-composites are examined. FG material properties is considered in thickness direction for the thermal responses of the composite. The equivalent material properties are obtained using Halphin-Tsai nano-mechanical model for composite layers. Moreover, effects of nano-scale sizes are taken into account employing FMCS. In this regard, for the first time, it is demonstrated that at certain values of GPL weight fraction the thermal bucking occurs. In obtaining results of vibrational behavior, both analytical solution and DNN methods are used.
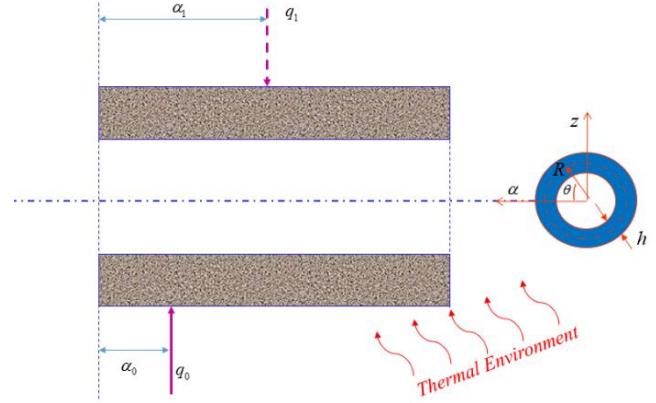

Fig. 1 Schematic representation of cylindrical nano-shell composite under thermal and dynamic loads with different lamina configuration

2. matematical model

The geometry of the model utilized in this study is schematically depicted in Figure 1. In this figure, a cylindrical shell with length L, middle surface radius R, and shell thickness h under thermal and dynamic loads is shown. The dynamic load q_0 is a transverse load.

As seen in Fig. 2, the shell is composed of multi-layer composite material with different lamina configurations defined as (Habibi *et al.* 2017, Safarpour *et al.* 2018, Habibi *et al.* 2019d, Ghazanfari *et al.* 2020, Jermsittiparsert *et al.* 2020, Safarpour *et al.* 2020)

$$\text{Pattern No. 1:} \quad GPL-U: \quad V_{GPL}(k) = V_{GPL}^* \tag{1}$$

$$\text{Pattern No. 2 } GPL-X: \quad V_{GPL}(k) = 2V_{GPL}^* \left|2k-1-N_L\right|/N_L \tag{2}$$

$$\text{Pattern No. 3:}$$
$$GPL-O: \quad V_{GPL}(k) = 2V_{GPL}^*\left[1-\left(\left|2k-1-N_L\right|/N_L\right)\right] \tag{3}$$

$$\text{Pattern No. 4:} \quad GPL-A: \quad V_{GPL}(k) = 2V_{GPL}^*(2k-1)/N_L \tag{4}$$

In the above equations, k determines the number of layers, V_{GPL}^* indicates the overall GPL volume fraction and N_L is the total number of layers. Moreover, V_{GPL}^* can be obtained from weight fraction g_{GPL} using densities of GPL and matrix as follows(Ebrahimi *et al.* 2019b, Ebrahimi *et al.* 2019c, Mohammadgholiha *et al.* 2019, Mohammadi *et al.* 2019, Ebrahimi *et al.* 2020b, Habibi *et al.* 2020, Shariati *et al.* 2020b, Shokrgozar *et al.* 2020b)

$$V_{GPL}^* = \frac{g_{GPL}}{g_{GPL}+(\rho_{GPL}/\rho_m)(1-g_{GPL})} \tag{5}$$

where ρ_m is the density of matrix and ρ_{GPL} represents the density of the GPL. The equivalent elastic modulus E of the reinforced composite is obtained using Halpin-Tsai model. The equations pertaining to this method is given in the following relations for randomly dispersed GPL (Affdl and Kardos 1976)
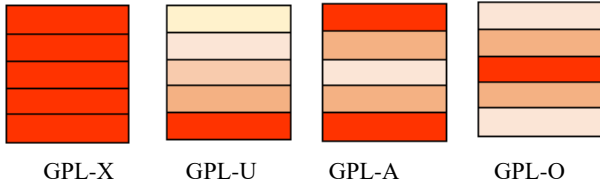
GPL-X   GPL-U   GPL-A   GPL-O

Fig. 2. Various patterns of composite structure

$$E = \frac{3}{8}E_L + \frac{5}{8}E_T,$$
$$E_L = \frac{1 + \xi_L n_L V_{GPL}}{1 - n_L V_{GPL}} E_m, \quad E_T = \frac{1 + \xi_T n_T V_{GPL}}{1 - n_T V_{GPL}} E_m \quad (6)$$

where E_T is the transverse elastic modulus of unidirectional composite layer and E_L is the longitudinal elastic modulus.

The parameters ξ_L and ξ_T are geometry factors defined in the following equations alongside with other undefined parameters(Hashemi *et al.* 2019, Moayedi *et al.* 2019, Moayedi *et al.* 2020b, Moayedi *et al.* 2020c, Oyarhossein *et al.* 2020, Shariati *et al.* 2020c)

$$\xi_L = 2(\mathbb{Z}_{GPL} / h_{GPL}), \quad \xi_t = 2(b_{GPL} / h_{GPL}),$$
$$n_L = \frac{(E_{GPL} - E_m / E_m)}{(E_{GPL} / E_m) + \xi_L}, \quad n_T = \frac{(E_{GPL} - E_m / E_m)}{(E_{GPL} / E_m) + \xi_T} \quad (7)$$

where average thickness, width, and length of the GPL is represented by h_{GPL}, b_{GPL} and $\mathbb{Z}_{GPL}$. Utilizing rule of mixture, the following mechanical constants of the GPL-reinforced nano-composite is obtained (Hashemi *et al.* 2019, Al-Furjan *et al.* 2020b, Cheshmeh *et al.* 2020, Lori *et al.* 2020, Najaafi *et al.* 2020, Shariati *et al.* 2020d)

$$\bar{E} = E_{GPL} V_{GPL} + E_M V_M,$$
$$\bar{\rho} = \rho_{GPL} V_{GPL} + \rho_M V_M,$$
$$\bar{v} = v_{GPL} V_{GPL} + v_M V_M,$$
$$\bar{\alpha} = \alpha_{GPL} V_{GPL} + \alpha_M V_M. \quad (8)$$

The displacement components in the FSDT is given by the following relations (Al-Furjan *et al.* 2020c, Al-Furjan *et al.* 2020d, Al-Furjan *et al.* 2020e, Bai *et al.* 2020, Zhang *et al.* 2020, Zhong *et al.* 2020, Guo *et al.* 2021a, Liu *et al.* 2021a)

$$u(\alpha, z, \theta, t) = u_m(\alpha, \theta, t) + z u_1(\alpha, \theta, t)$$
$$v(\alpha, z, \theta, t) = v_m(\alpha, \theta, t) + z v_1(\alpha, \theta, t) \quad (9)$$
$$w(\alpha, z, \theta, t) = w_m(\alpha, \theta, t)$$

In these relations, the components $u_m(\alpha, \theta, t)$, $v_m(\alpha, \theta, t)$ and $w_m(\alpha, \theta, t)$ represent the axial, circumferential and radial displacement on the middle surface of the cylindrical shell. The two components $u_1(\alpha, \theta, t)$ and $v_1(\alpha, \theta, t)$ are the rotation angle in the axial and circumferential directions for the normal of the middle surfaces with respect to normal position. Moreover, the stress components for the cylindrical shell can be expressed as functions of strains cylindrical coordinate system

$$\begin{bmatrix} \sigma_{\alpha\alpha} \\ \sigma_{\theta\theta} \\ \sigma_{zz} \\ \sigma_{\alpha\theta} \\ \sigma_{\alpha z} \\ \sigma_{\theta z} \end{bmatrix} = \begin{bmatrix} \bar{Q}_{11} & \bar{Q}_{12} & \bar{Q}_{13} & 0 & 0 & 0 \\ \bar{Q}_{12} & \bar{Q}_{22} & \bar{Q}_{23} & 0 & 0 & 0 \\ \bar{Q}_{13} & \bar{Q}_{23} & \bar{Q}_{33} & 0 & 0 & 0 \\ 0 & 0 & 0 & \bar{Q}_{44} & 0 & 0 \\ 0 & 0 & 0 & 0 & \bar{Q}_{55} & 0 \\ 0 & 0 & 0 & 0 & 0 & \bar{Q}_{66} \end{bmatrix} \begin{bmatrix} \varepsilon_{\alpha\alpha} \\ \varepsilon_{\theta\theta} \\ \varepsilon_{zz} \\ \varepsilon_{\alpha\theta} \\ \varepsilon_{\alpha z} \\ \varepsilon_{\theta z} \end{bmatrix} \quad (10)$$

The coefficients in Eq. (12) is presented in detail by ref (Barooti *et al.* 2017). In order to extract equations of motion the principle of minimum potential energy is employed as (Adamian *et al.* 2020, Al-Furjan *et al.* 2020f, Al-Furjan *et al.* 2020g, Li *et al.* 2020; Shi et al. 2020; Zare *et al.* 2020, Dai *et al.* 2021a, Zhang *et al.* 2021)

$$\int_{t_1}^{t_2} (\delta T - \delta U + \delta W_1 - \delta W_2) dt = 0 \quad (11)$$

where, U represents the internal strain energy in the modified couple stress theory (MCST) which is given by the following relation(Liu *et al.* 2020a, Habibi *et al.* 2021a, He *et al.* 2021, Huang *et al.* 2021a, Huo *et al.* 2021, Liu *et al.* 2021b, Zhang *et al.* 2021)

$$U = \frac{1}{2} \iiint_V (\sigma_{ij} \varepsilon_{ij} + m_{ij}^s \chi_{ij}^s) R \, dx d\theta dz \quad (12)$$

In addition to stress and strain tensors components σ_{ij} and ε_{ij}, the components of symmetric rotation gradient tensor χ_{ij}^s and higher-order stress tensor m_{ij}^s are also affect the internal energy

$$\chi_{ij}^s = \frac{1}{2}(\varphi_{i,j} + \varphi_{j,i})$$
$$m_{ij}^s = 2l^2 \mu \chi_{ij}^s \quad (13)$$

In which l and φ_{ij} represent MCST and the small rotation vector components. The parameter l for a composite material can be expressed as(Liu *et al.* 2020a, Wang *et al.* 2020, Zhou *et al.* 2020, Dai *et al.* 2021b, Guo *et al.* 2021b, Peng *et al.* 2021, Shao *et al.* 2021, Wu and Habibi 2021b)

$$l = l_{GPL} V_{GPL} + l_M V_M \quad (14)$$

In addition, the non-zero components of symmetric rotation gradient tensor are given by (Zhao *et al.* 2021, Ebrahimi and Safarpour 2018, Dai and Safarpour 2021c, Huang *et al.* 2021b, Jiao *et al.* 2021, Moradi *et al.* 2021, Wang *et al.* 2021, Xu *et al.* 2021, Zhang *et al.* 2021, Zhao *et al.* 2021)

$$\chi_{\alpha\alpha}^s = -\frac{1}{2}\left(\frac{\partial v_1}{\partial \alpha} + \frac{1}{R}\frac{\partial v}{\partial \alpha} - \frac{1}{R}\frac{\partial^2 w}{\partial \alpha \partial \theta}\right)$$
$$\chi_{\theta\theta}^s = -\frac{1}{2R}\left(\frac{1}{R}\frac{\partial u}{\partial \theta} - \frac{\partial v_m}{\partial \alpha} - z\frac{\partial v_1}{\partial \alpha}\right) - \frac{1}{2}\left(\frac{1}{R}\frac{\partial^2 w}{\partial \alpha \partial \theta} - \frac{1}{R}\frac{\partial u_1}{\partial \theta}\right)$$
$$\chi_{zz}^s = -\frac{1}{2}\left(\frac{1}{R}\frac{\partial u_1}{\partial \theta} - \frac{\partial v_1}{\partial \alpha} - \frac{1}{R^2}\frac{\partial u}{\partial \theta}\right)$$
$$\chi_{\alpha\theta}^s = -\frac{1}{4}\left(\frac{1}{R^2}\frac{\partial v}{\partial \theta} + \frac{\partial^2 w}{\partial \alpha^2} - \frac{1}{R^2}\frac{\partial^2 w}{\partial \theta^2} - \frac{\partial u_1}{\partial \alpha} + \frac{1}{R}\frac{\partial v_1}{\partial \theta}\right)$$
$$\chi_{\alpha z}^s = -\frac{1}{4}\left(\frac{1}{R}\frac{\partial^2 u}{\partial \alpha \partial \theta} - \frac{\partial^2 v}{\partial \alpha^2} - \frac{v}{R^2} + \frac{1}{R^2}\frac{\partial w}{\partial \theta} + \frac{v_1}{R}\right) - \frac{z}{4}\left(\frac{1}{R}\frac{\partial^2 v_1}{\partial \alpha \partial \theta} - \frac{\partial^2 v_1}{\partial \alpha^2}\right)$$
$$\chi_{\theta z}^s = -\frac{1}{4}\left(\frac{1}{R^2}\frac{\partial^2 u}{\partial \theta^2} - \frac{1}{R}\frac{\partial^2 v}{\partial \alpha \partial \theta} - \frac{1}{R}\frac{\partial w}{\partial \alpha} + \frac{u_1}{R}\right) - \frac{z}{4}\left(\frac{1}{R^2}\frac{\partial^2 u_1}{\partial \theta^2} - \frac{1}{R}\frac{\partial^2 v_1}{\partial \alpha \partial \theta}\right) \quad (15)$$

At last, the classical and non-classical parts of strain energy in FMCS parameter can be calculated using the following relations

$$\frac{1}{2}\iiint_V (\sigma_{ij}\delta\varepsilon_{ij})dV = \iint_A \left\{ \begin{array}{l} (N_{\alpha\alpha}\frac{\partial}{\partial\alpha}\delta u_0 + M_{\alpha\alpha}\frac{\partial}{\partial\alpha}\delta u_1) \\[4pt] + N_{\theta\theta}(\frac{1}{R}\frac{\partial}{\partial\theta}\delta v_0 + \frac{\delta w_0}{R}) + \\[4pt] M_{\theta\theta}\frac{1}{R}\frac{\partial}{\partial\theta}\delta v_1 + Q_{\alpha z}(\delta u_1 + \frac{\partial}{\partial\alpha}\delta w_m) + \\[4pt] N_{\alpha\theta}(\frac{1}{R}\frac{\partial}{\partial\theta}\delta u_m + \frac{\partial}{\partial\alpha}\delta v_m) \\[4pt] + M_{\alpha\theta}(\frac{1}{R}\frac{\partial}{\partial\theta}\delta u_1 + \frac{\partial}{\partial\alpha}\delta v_1) \\[4pt] + Q_{z\theta}(\delta v_1 + \frac{1}{R}\frac{\partial}{\partial\theta}\delta w_m - \frac{\delta v_m}{R}) \end{array} \right\} Rd\alpha d\theta$$

$$\frac{1}{2}\iiint_V (m_{ij}^s \delta\chi_{ij}^s)dV = \iint_A \left\{ \begin{array}{l} (-\frac{Y_{\theta\theta}}{2R^2} + \frac{Y_{zz}}{2R^2})\frac{\partial}{\partial\theta}\delta u_m \\[4pt] -\frac{Y_{zx}}{2R}\frac{\partial^2}{\partial\theta\partial\alpha}\delta u_m - (\frac{Y_{\theta z}}{2R})\frac{\partial^2}{\partial\theta^2}\delta u_m \\[4pt] +(\frac{Y_{\theta\theta}}{2R} - \frac{Y_{\alpha\alpha}}{2R})\frac{\partial}{\partial\alpha}\delta v_m + (\frac{Y_{\alpha z}}{2})\frac{\partial^2}{\partial\alpha^2}\delta v_m \\[4pt] -(\frac{Y_{\theta\alpha}}{2R^2})\frac{\partial}{\partial\theta}\delta v_m + (\frac{Y_{\theta z}}{2R})\frac{\partial}{\partial\alpha}\delta w_m \\[4pt] +(\frac{Y_{\theta z}}{2R})\frac{\partial^2}{\partial\theta\partial\alpha}\delta v_m + (\frac{Y_{\alpha z}}{2R^2})\delta v_m \\[4pt] -(\frac{Y_{\theta\alpha}}{2})\frac{\partial^2}{\partial\alpha^2}\delta w_m \\[4pt] -(\frac{Y_{z\alpha}}{2R^2})\frac{\partial}{\partial\theta}\delta w_m + (\frac{Y_{\alpha\theta}}{2R^2})\frac{\partial^2}{\partial\theta^2}\delta w_m + \\[4pt] \frac{Y_{\theta\theta}}{2R} + \frac{Y_{\alpha\alpha}}{2R})\frac{\partial^2}{\partial\theta\partial\alpha}\delta w_m \\[4pt] +(\frac{Y_{\alpha\theta}}{2})\frac{\partial}{\partial\alpha}\delta u_1 + (\frac{Y_{\theta\theta}}{2R} - \frac{Y_{\alpha\alpha}}{2R})\frac{\partial}{\partial\theta}\delta u_1 \\[4pt] -\frac{T_{z\alpha}}{2R}\frac{\partial^2}{\partial\theta\partial\alpha}\delta u_1 \\[4pt] -(\frac{Y_{z\theta}}{2R})\delta u_1 - (\frac{Y_{\alpha\theta}}{2R})\frac{\partial}{\partial\theta}\delta v_1 + \\[4pt] (\frac{Y_{\theta\theta}}{2R} - \frac{Y_{\alpha\alpha}}{2} + \frac{Y_{zz}}{2})\frac{\partial}{\partial\alpha}\delta v_1 \\[4pt] +\frac{T_{z\theta}}{2R}\frac{\partial^2}{\partial\theta\partial\alpha}\delta v_1 - (\frac{T_{z\theta}}{2R^2})\frac{\partial^2}{\partial\theta^2}\delta u_1 \\[4pt] +(\frac{T_{\alpha z}}{2})\frac{\partial^2}{\partial\alpha^2}\delta v_1 - \frac{Y_{\alpha z}}{2R}\delta v_1 \end{array} \right\} Rdxd\theta \quad (16)$$

The given unknown parameters are defined in the following relations

$$(N_{\alpha\alpha}, N_{\theta\theta}, N_{\alpha\theta}) = \int_{-h/2}^{h/2} (\sigma_{\alpha\alpha}, \sigma_{\theta\theta}, \sigma_{\alpha\theta})dz,$$
$$(M_{\alpha\alpha}, M_{\theta\theta}, M_{\alpha\theta}) = \int_{-h/2}^{h/2} (\sigma_{\alpha\alpha}, \sigma_{\theta\theta}, \sigma_{\alpha\theta})zdz,$$
$$(Q_{\alpha z}, Q_{z\theta}) = \int_{-h/2}^{h/2} k_s(\sigma_{\alpha z}, \sigma_{z\theta})dz, \quad (17)$$
$$(Y_{\alpha\alpha}, Y_{\theta\theta}, Y_{zz}, Y_{\alpha\theta}, Y_{\alpha z}, Y_{z\theta}) = \int_{-h/2}^{h/2} (m_{\alpha\alpha}, m_{\theta\theta}, m_{zz}, m_{\alpha\theta}, m_{\alpha z}, m_{z\theta})dz,$$
$$(T_{\alpha\alpha}, T_{\theta\theta}, T_{zz}, T_{\alpha\theta}, T_{\alpha z}, T_{z\theta}) = \int_{-h/2}^{h/2} (m_{\alpha\alpha}, m_{\theta\theta}, m_{zz}, m_{\alpha\theta}, m_{\alpha z}, m_{z\theta})zdz$$

The first energy term is Eq. (11) is the kinetic energy which can be expressed as following relation in cylindrical coordinate system (Ma *et al.* 2021, SafarPour and Ghadiri 2017, SafarPour *et al.* 2017; SafarPour *et al.* 2017, Hou *et al.* 2021, Huang *et al.* 2021c, Liu *et al.* 2021b, Yu *et al.* 2022)

$$\delta T = \iint_Z \iint_A \rho \left\{ \begin{array}{l} (\frac{\partial u_m}{\partial t} + z\frac{\partial u_1}{\partial t})(\frac{\partial}{\partial t}\delta u_m + z\frac{\partial}{\partial t}\delta u_1) \\[4pt] +(\frac{\partial v_m}{\partial t} + z\frac{\partial v_1}{\partial t})(\frac{\partial}{\partial t}\delta v_m + z\frac{\partial}{\partial t}\delta v_1) \\[4pt] +(\frac{\partial w}{\partial t})\frac{\partial}{\partial t}\delta w \end{array} \right\} Rdz d\alpha d\theta \quad (18)$$

The temperature is assumed to be varied in the thickness of the shell. Therefore, the energy from the temperature distribution can be expressed as (Al-Furjan *et al.* 2020h, Al-Furjan *et al.* 2020i, Al-Furjan *et al.* 2020j, Al-Furjan *et al.* 2020k, Al-Furjan *et al.* 2020l, Al-Furjan *et al.* 2020n, Al-Furjan *et al.* 2020m, Al-Furjan *et al.* 2020p, Al-Furjan *et al.* 2020q)

$$W_1 = \frac{1}{2}\iint_A \left[N_1^T(\frac{\partial w_m}{\partial\alpha})^2 + N_2^T(\frac{\partial v_m}{\partial\alpha})^2 \right] Rd\alpha d\theta \quad (19)$$

In which, the resultants of thermal load are N_1^T and N_2^T given by the following relations (Pandit *et al.* 2020, Shi *et al.* 2021)

$$N_1^T = \int_{-h/2}^{h/2} (\bar{Q}_{11} + \bar{Q}_{12} + \bar{Q}_{13})\beta(T - T_0)dz,$$
$$N_2^T = \int_{-h/2}^{h/2} (\bar{Q}_{21} + \bar{Q}_{22} + \bar{Q}_{23})\beta(T - T_0)dz. \quad (20)$$

Moreover, the components of the thermal expansion in different directions are

$$\beta = [\beta_{xxe} \ \beta_{\theta\theta e} \ \beta_{zze} \ 0 \ 0 \ 0]^T \quad (21)$$

Assuming perfect bonding between layers and linear distribution of temperature in the thickness the following relation can be applied for the temperature variation in the shell thickness (Shahsiah and Eslami 2003)

$$T = T_i - (T_i - T_o)\left(\frac{i-1}{N_L-1}\right) \quad (22)$$

where N_L is the total number of layers and i is the number of layer. The term W_2 is the energy corresponding to the applied dynamic force $q_{dynamic}$

$$W_2 = \frac{1}{2}\{q_{dynamic}w^2\}RdV \quad (23)$$

Definitions of all terms in Eq. (11) are now determined in detail in Eqs. (12), (18), (19) and (23). Substituting these relations into Eq. (11) and integrating considering the boundary conditions results in

$$\left[\frac{\partial N_{\alpha\alpha}}{\partial\alpha} + \frac{1}{R}\frac{\partial N_{\alpha\theta}}{\partial\theta} + \frac{1}{2R^2}(-\frac{\partial Y_{\theta\theta}}{\partial\theta} + \frac{\partial Y_{zz}}{\partial\theta}) + \frac{1}{2R}\frac{\partial^2 Y_{z\alpha}}{\partial\alpha\partial\theta} + \frac{1}{2R^2}\frac{\partial^2 Y_{\theta z}}{\partial\theta^2} \right]\delta u_0$$

$$+ \left[\frac{\partial N_{\alpha\theta}}{\partial\alpha} + \frac{1}{R}\frac{\partial}{\partial\theta}N_{\theta\theta} + \frac{Q_{z\theta}}{R} + \frac{1}{2}\left\{ \begin{array}{l} \frac{1}{R}\frac{\partial}{\partial\alpha}(-Y_{\alpha\alpha} + Y_{\theta\theta}) \\[4pt] -\frac{1}{R^2}\frac{\partial Y_{\theta\alpha}}{\partial\theta} - \frac{\partial^2 Y_{\alpha z}}{\partial\alpha^2} - \frac{Y_{zz}}{R^2} - \frac{1}{R}\frac{\partial^2 Y_{z\theta}}{\partial\theta\partial x} \end{array} \right\} \right]\delta v_0$$

$$-N_2^T\frac{\partial^2 v_m}{\partial\alpha^2}\delta v_m + \left[\begin{array}{l} \frac{\partial Q_{\alpha z}}{\partial\alpha} + \frac{1}{R}\frac{\partial Q_{z\theta}}{\partial\theta} - \frac{N_{\theta\theta}}{R} - \frac{1}{2R^2}\frac{\partial^2 Y_{\theta z}}{\partial\theta^2} \\[4pt] -\frac{1}{2R^2}\frac{\partial Y_{z\alpha}}{\partial\theta} + \frac{1}{2R}\frac{\partial Y_{\theta z}}{\partial\alpha} + \frac{\partial^2 Y_{\alpha\theta}}{2\partial\alpha^2} \end{array} \right]\delta w_m$$

$$+ \left[-\frac{1}{2R}\frac{\partial^2}{\partial\theta\partial\alpha}(Y_{\alpha\alpha} - Y_{\theta\theta}) - N_1^T\frac{\partial^2 w}{\partial\alpha^2} \right]\delta w_m + \left[\begin{array}{l} \frac{\partial M_{\alpha\alpha}}{\partial\alpha} + \frac{1}{R}\frac{\partial M_{\theta\theta}}{\partial\theta} - Q_{\alpha z} \\[4pt] + \frac{1}{2}\frac{\partial Y_{\alpha\theta}}{\partial\alpha} - \frac{1}{2R}\frac{\partial}{\partial\theta}(Y_{zz} - Y_{\theta\theta}) \end{array} \right]\delta u_1 \quad (24)$$

$$+ \left[\frac{Y_{zz}}{R} + \frac{1}{2R}\frac{\partial^2 T_{\alpha z}}{\partial\theta\partial\alpha} + \frac{1}{2R^2}\frac{\partial^2 T_{\alpha\theta}}{\partial\theta^2} \right]\delta u_1 + \left[\begin{array}{l} \frac{1}{R}\frac{\partial M_{\theta\theta}}{\partial\theta} + \frac{\partial M_{\alpha\theta}}{\partial\alpha} - Q_{z\theta} \\[4pt] + \frac{1}{2}\frac{\partial}{\partial\alpha}(Y_{zz} - Y_{xx} + \frac{T_{\theta\theta}}{R}) \end{array} \right]\delta v_1$$

$$+ \left[-\frac{1}{2}\frac{\partial Y_{\theta z}}{\partial\theta} + \frac{Y_{\alpha z}}{2R} - \frac{1}{2R}\frac{\partial^2 T_{\theta z}}{\partial\theta\partial\alpha} - \frac{1}{2}\frac{\partial^2 T_{\alpha z}}{\partial\alpha^2} \right]\delta v_1 = \left\{ I_0\frac{\partial^2 u_m}{\partial t^2} + I_1\frac{\partial^2 u_1}{\partial t^2} \right\}\delta u_m$$

$$+ \left\{ I_0\frac{\partial^2 v_m}{\partial t^2} + I_1\frac{\partial^2 v_1}{\partial t^2} \right\}\delta v_m + I_0\frac{\partial^2 w_m}{\partial t^2}\delta w_m + \left\{ I_1\frac{\partial^2 u_m}{\partial t^2} + I_2\frac{\partial^2 u_1}{\partial t^2} \right\}\delta u_1$$

$$+ \left\{ I_1\frac{\partial^2 v_m}{\partial t^2} + I_2\frac{\partial^2 v_1}{\partial t^2} \right\}\delta v_1 + q_{dynamic}\delta w_m = 0$$

3. Solution strategy

Governing equations in Eq. (24) are now solved using analytical methods for the cylindrical composite shell obeying coupled stress theory. The simply supported boundary condition is assumed in the ends of the shell at $\alpha = 0, L$ and $\theta = \frac{\pi}{2}, \frac{3\pi}{2}$. Regarding these boundary conditions, a consistent displacement field based on Fourier series expansion can be obtained as

$$\begin{Bmatrix} u_0(\alpha,\theta,t) \\ v_0(\alpha,\theta,t) \\ w_0(\alpha,\theta,t) \\ u_1(\alpha,\theta,t) \\ v_1(\alpha,\theta,t) \end{Bmatrix} = \sum_{m=1}^{\infty}\sum_{n=1}^{\infty} \begin{Bmatrix} U_{0mn}\cos(\frac{m\pi}{L}\alpha)\cos(n\theta) \\ V_{0mn}\sin(\frac{m\pi}{L}\alpha)\sin(n\theta) \\ W_{0mn}\sin(\frac{m\pi}{L}\alpha)\cos(n\theta) \\ U_{1mn}\cos(\frac{m\pi}{L}\alpha)\cos(n\theta) \\ V_{1mn}\sin(\frac{m\pi}{L}\alpha)\sin(n\theta) \end{Bmatrix}\sin(\omega t) \quad (25)$$

in which the coefficients $\{U_{0mn}, V_{0mn}, W_{0mn}, U_{1mn}, V_{1mn}\}$ have to be calculated based on the given governing equations. The integer numbers n and m are the wavenumbers in circumferential and axial directions, respectively. Substituting Eq. (25) into Eq. (24) gives (Al-Furjan *et al.* 2020r, Al-Furjan *et al.* 2020w, Al-Furjan *et al.* 2020t, Al-Furjan *et al.* 2020u, Al-Furjan *et al.* 2020v, Al-Furjan *et al.* 2020w, Al-Furjan *et al.* 2020x, Al-Furjan *et al.* 2021a, Al-Furjan *et al.* 2021b)

$$\left(\begin{bmatrix} K_{11} & K_{12} & K_{13} & K_{14} & K_{15} \\ K_{21} & K_{22} & K_{23} & K_{24} & K_{25} \\ K_{31} & K_{32} & K_{33} & K_{34} & K_{35} \\ K_{41} & K_{42} & K_{43} & K_{44} & K_{45} \\ K_{51} & K_{52} & K_{53} & K_{54} & K_{55} \end{bmatrix} - \omega_{ex}^2 \begin{bmatrix} M_{11} & M_{12} & M_{13} & M_{14} & M_{15} \\ M_{21} & M_{22} & M_{23} & M_{24} & M_{25} \\ M_{31} & M_{32} & M_{33} & M_{34} & M_{35} \\ M_{41} & M_{42} & M_{43} & M_{44} & M_{45} \\ M_{51} & M_{52} & M_{53} & M_{54} & M_{55} \end{bmatrix}\right) \begin{Bmatrix} U_0 \\ V_0 \\ W_0 \\ U_1 \\ V_1 \end{Bmatrix} = \begin{bmatrix} 0 \\ 0 \\ q_{dynamic} \\ 0 \\ 0 \end{bmatrix} \begin{Bmatrix} U_0 \\ V_0 \\ W_0 \\ U_1 \\ V_1 \end{Bmatrix} \quad (26)$$

where K_{ij} and M_{ij} are the components of the stiffness and matrices, respectively. In Eq. (26), the excitation frequency is denoted by ω_{ex}. Finally, and applied dynamic load ($q_{dynamic}$) is expressed as

$$q_{dynamic} = \sum_{m=1}^{\infty}\sum_{n=1}^{\infty} q_0 \sin(\frac{m\pi}{L}\alpha)\cos(n\theta)\sin(\omega t), \quad (27)$$

Solving Eq. (27) determines two unknowns of the equation: the excitation frequency and deflection of the beam under dynamics loads. Moreover, the following dimensionless parameters are defined for forced vibration amplitude and excitation frequency to be utilized in the next sections

$$\Omega = 10 \times \omega_{ex} L \sqrt{\rho/E}, \quad \overline{W}_{uniform} = W_{0mn}\frac{10Eh^3}{L^4 q_0} \quad (28)$$

4. Validation

The results of solving the developed governing equation is presented in Table 1 for different thickness adopted from

Beni *et al.* (Tadi Beni *et al.* 2016). The obtained results are also compared to the results presented in the literature to validate the procedure of solving in the present paper. As can be observed, an acceptable agreement exists between results of the two study for the first three natural frequency of the cylindrical shell Ref (Tadi Beni *et al.* 2016).

4.1 Deep learning models

The natural frequencies in this study is obtained by solving linear equations with high computational costs. Thus, in the case of sufficient available data, the deep learning method can be utilized with acceptable accuracy and very low computational costs. Therefore, a neural network is designed in this study to analyzed effects of various parameters. These type of neural networks are composed of perceptrons each has input and output values. At each perceptron, the input values are weighted and biased to give output. The overall network's output is compared to the actual output obtained by solving nonlinear equations. The comparison parameter is mean squared value (MSE):

$$\text{MSE} = \frac{1}{n}\sum_{i=1}^{n}(Y-\hat{Y})^2 \quad (29)$$

The weight and bias values were then adjusted using ADADELTA method to obtain the minimum value for MSE. The details of this method and theoretical background can be found in Ref. (Yegnanarayana 2009). Once the MSE reaches its minimum value, the weight and bias values are finalized, and the neural network is considered as the trained network.

4.1.1 Optimization by ADADELTA to adjust the DNN parameters

The ADADELTA method mentioned in the previous section is an optimization method to minimize MSE which has some merits in comparison to other methods. To name some:

- The learning rate parameter in this method is determined automatically.
- Hyperparameters has of influence on the ADADELTA performance.
- Both distributed and local environments are used.

At each iteration (epoch) the weight and bias values of all network is updated using the following procedure

$$\chi_{t+1} = \chi_t + \nabla\chi_t$$
$$\nabla\chi_t = -\eta\frac{\partial f(\chi_t)}{\partial\chi_t} \quad (30)$$

where, initial learning rate is represented by η. In the following, the notation G_t is used instead of $\frac{\partial f(\chi_t)}{\partial\chi_t}$ for the t-th epoch. The root mean square (RMS) is used to update values of weights and biases

$$\text{RMS}[G_t] = \sqrt{E[G_t^2] + \varepsilon} \quad (31)$$

In this relation, ε is a constant. Squared gradient has

Table 4 Dependency of natural frequency in a cylindrical shell made of GPL-composite on the temperature change, GPL pattern, and geometrical parameters

| | | ΔT =10K | | ΔT =20K | | ΔT =30K | |
		h/R=0.08	h/R=0.1	h/R=0.08	h/R=0.1	h/R=0.08	h/R=0.1
GPL-U	*l/R*						
	0	1.948752	1.982586	1.904938	1.973578	1.859902	1.964363
	1/3	2.070645	2.102498	2.028391	2.092946	1.985038	2.083173
	1/2	2.184729	2.214933	2.143707	2.204870	2.101676	2.194574
	2/3	2.302991	2.331662	2.263052	2.321068	2.222178	2.310231
GPL-X	*l/R*						
	0	1.947517	1.981282	1.903786	1.972283	1.858836	1.963078
	1/3	2.069517	2.101302	2.027344	2.091759	1.984077	2.081997
	½	2.183646	2.213784	2.142704	2.203735	2.100757	2.193447
	2/3	2.301909	2.330516	2.262047	2.319933	2.221255	2.309107
GPL-O	*l/R*						
	0	1.951057	1.984761	1.907392	1.975764	1.862513	1.966560
	1/3	2.072872	2.104606	2.030755	2.095065	1.987547	2.085304
	1/2	1.186938	2.217031	2.146045	2.206980	2.104149	2.196697
	2/3	2.305233	2.333800	2.265415	2.323218	2.224670	2.312393
GPL-A	*l/R*						
	0	1.949577	1.983336	1.905848	1.974335	1.860901	1.965126
	1/3	2.073030	2.104788	2.030885	2.095243	1.987647	2.085479
	1/2	2.188392	2.218488	2.147493	2.208434	2.105592	2.198148
	2/3	2.307948	2.336501	2.268143	2.325918	2.227411	2.315091

the expected value of $E\left[G_t^2\right]$ obtained from the following equation using decay rate ρ

$$E\left[G_t^2\right] = \rho E\left[G_{t-1}^2\right] + (1-\rho)G_t^2 \tag{32}$$

The adjustment in each epoch can be calculated now using Eqs. (31) and (32) as follows

$$\nabla \chi_t = -\frac{\eta}{RMS\left[G_t\right]}G_t \tag{33}$$

According to Zeiler (2012), ADADELTA optimizer has the highest performance in minimizing errors in classification of handwriting digits provided by MNIST. After training the DNN model, some predictions are conducted using this trained model. Table 2 presents results of the DNN model for various values of g_{GPL}, l/R and MSN parameters. According to these results, it is concluded that having higher values of g_{GPL} and MSN leads to better responses are prediction.

5. Results and discussion

Frequency and vibrational stability analyses results are presented in this section for cylindrical shell made of GPL-reinforced composite with $L_{GPL} = 2.5\ nm$, $h_{GPL} = 1.5\ nm$ and $R_{GPL} = 0.75\ nm$ under thermal and dynamical loading. In this regard, the effect of different parameters is investigated to observe frequency change and excitation frequencies in different conditions. Some of the material properties of the GPL are assumed to be dependent on temperature (Wu *et al.* 2017):
$E = (3.52 - 0.0034T)\ GPa$ and $\alpha_m = 45(1 + 0.0005\Delta T) \times 10^{-6}/K$ in which $T = T_0 + \Delta T$.

Other materials properties are presented in Table 3. Influence of number of layers N_L on the relative natural frequencies in different lamina patterns is depicted in Figure 3. As can be observed, the relative frequencies of pattern 1 and 4 is unaffected by changes in number of layers. However, the other two patterns, i.e., patterns 2 and 3, are affected by change in number of layers. Pattern 3 shows a rise relative frequency with increase in number of layers up to $N_L = 7$. Afterwards, the frequency virtually remains constant. An inverse response in seen in the pattern 2 in which with increase in number of layers the relative frequency decreases. At $N_L = 7$, the relative frequency becomes constant. This shows that for non-uniform distribution of the GPL in pattern 3 leads to stability of the structure when in pattern 2 it has a reverse effect. The overall feature of this figure is that at the high number of layers ($N_L > 7$), there is a low difference in the vibrational behavior of different layers.

The effect of mode number and weight fraction of GPL on the relative frequency is shown in Fig. 4. It is seen that increasing g_{GPL} results in increase in frequency of the cylindrical shell structure. Thus it can be concluded that the stability of the structure is improved with increase in weight fraction of GPL in laminated composite shells. On the hand, the mode number has a negligible effect on the relative frequency of the structure as all the curves coincide. However, with further observation in higher resolution, it is seen that a slight increase in relative frequency ratio with increase in mode numbers.
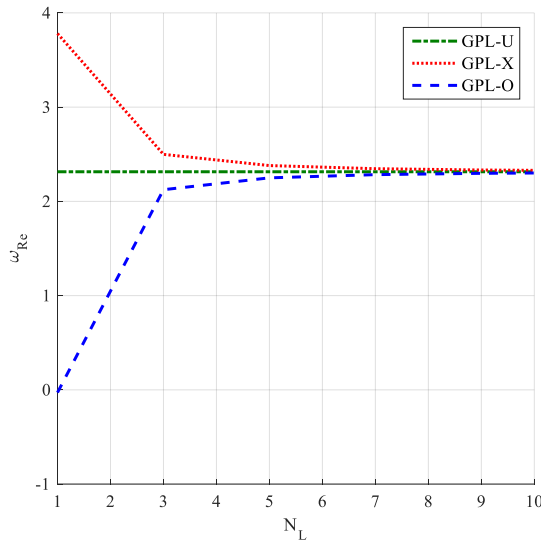
Fig. 3 Comparison of relative frequency ratio in different lamina patterns for various number of total layers N_L ($\Delta T = 10K$, l=R/3, Pattern2, L/R=10, R/h=10 and n=m=1)

Fig. 5 Resonance frequency as function of GPL weight fraction ($\Delta T = 20K$, l=R/3, Pattern2, L/R=10, R/h=10 and n=m=1)
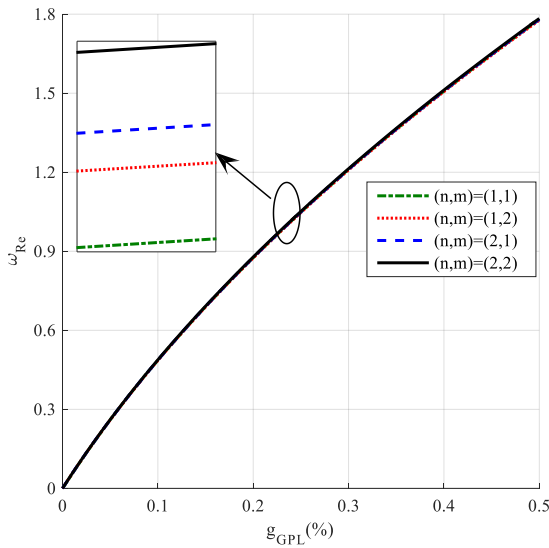

Fig. 4 Comparison of relative frequency ratio in different wavenumbers for various g_{GPL} ($\Delta T = 10K$, l=R/3, Pattern2, L/R=10, R/h=10)

Effects of temperature change ΔT and geometrical parameters h/R and l/R is presented in Table 4 for different GPL distribution configuration. It is seen that variations of GPL distribution pattern lead to different natural frequency values. Increase in l/R results in increase in natural frequencies in all temperature changes and patterns. Similarly, increase in h/R leads to rise in the natural frequencies in all scenarios. On the other hand, temperature change has reverse effect on the natural frequency. With rise in temperature change, the natural frequency decreases. For an account, increase in temperature change from 10K to 30K in GPL-U patterns for
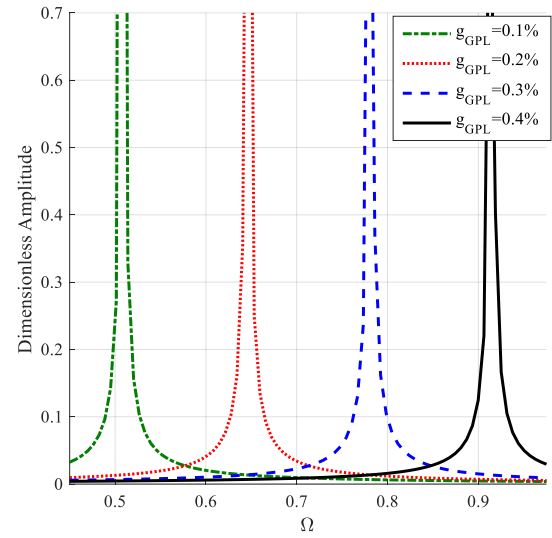
$l/R = 1/3$ and $h/R = 0.08$ leads to a decrease in natural frequency from 2.070645 to 1.985038, which is 4.3% reduction. The differences in the formulation procedure between classical and modified couples stress theories are depicted in Table 4 as functions of weight fraction of GPL g_{GPL} and temperature change ΔT. In these 3D plots it's observed that at a certain value of temperature change a spike in the relative natural frequency is seen in both MCS and classical theories. This phenomenon is due to buckling occurrence in the shell structure. It is seen that with employing MCST, the point where this spike happens move towards lower temperature changes. Thus, the effects of size-dependency are very important in prediction of buckling behavior under thermal loadings. Except for this point, on other temperature change range the relative natural frequency ratio increases with increase in temperature. The effect of weight fraction is similar in both theories. With rise in weight fraction in both cases the natural frequency increases. This behavior is somehow expectable because with increase in g_{GPL} results in increase in stiffness of the composite material which leads to increase in natural frequency in general manner. The dependency dimensionless excitation frequency and dynamic deflection on the g_{GPL} is shown in Fig. 5. The resonance occurrence is obvious in specific values of excitation frequency when the deflection tends to infinity. This excitation frequency increases with increase in the weight fraction of GPL. Increase in g_{GPL} generally increases the stiffness of the structure. Hence, the stability and resonance frequency also increase as a result of a rise in g_{GPL}.

GPL distribution patterns also considerably change the resonance behavior of the structure. As seen in Fig. 6, changing the pattern from GPL-A to GPL-O notably increases the resonance frequency. It is observed that GPL-
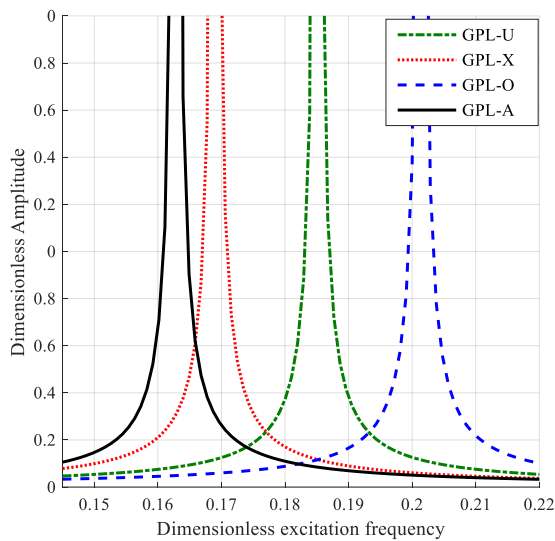
Fig. 6 Resonance frequency as function of GPL distribution pattern ($\Delta T = 20K$, l=R/3, L/R=10, R/h=10 and n=m=1)

Fig. 8 Resonance frequency as function of geometrical parameter ΔT (K) (l/R=0.5, Pattern2, L/R=10, R/h=10 and n=m=1)

stress in the modeling problems in this scale. Without using MCS theory such considerable changes in the resonance frequency cannot be screened.

Finally, effect of temperature changes ΔT on the resonance frequency of the structure is shown in Fig. 8. It is obvious that with increase in ΔT from 0 to 20K the non-dimensional resonance frequency slightly decrease from 0.377 to 0.371 (~1.6%). Although, amount of temperature changes reduces the resonance frequency, the change is not significant in this range of temperature change. However, as discussed before, with decrease in the stiffness of the structure the resonance frequency is also decreased. Higher temperature changes lead to lower stiffness of the materials in this study.
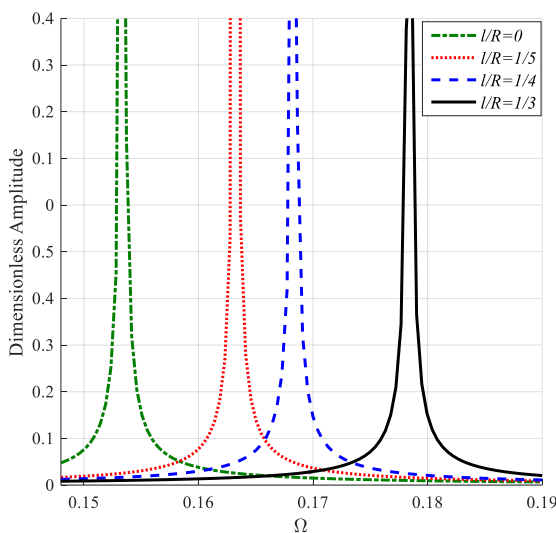

Fig. 7 Resonance frequency as function of geometrical parameter l/R ($\Delta T = 20K$, Pattern2, L/R=10, R/h=10 and n=m=1)

A has the lowest resonance frequency while GPL-O has the highest resonance frequency. Therefore, it is concluded that for better stability of the structure using GPL distribution pattern GPL-O is recommended. The resonance frequency of pattern GPL-A and GPL-X is very close to each other as a result of their similarity in the mathematical model used in this study.

Effect of geometrical parameter l/R on the resonance frequency of the structure is depicted in Fig. 7. It is obvious that with increase in l/R from 0 to 1/3 the non-dimensional resonance frequency increases from 0.153 to 0.178. This conclusion is a very important conclusion which is justifies the importance of employing modified couple
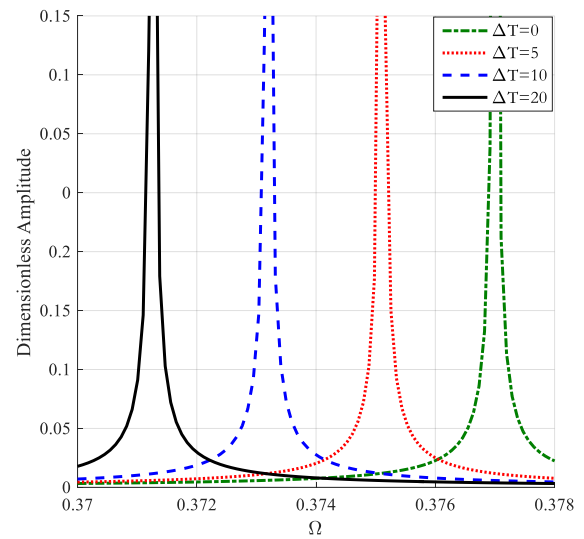
6. Conclusions

In this study, effects of thermal loadings on the buckling and resonance frequency of graphene reinforced nano-composites were examined. FG material properties were considered in thickness direction for the thermal responses of the composite. The equivalent material properties were obtained using Halphin-Tsai nano-mechanical model for composite layers. Moreover, effects of nano-scale sizes were taken into account employing FMCS parameter. Moreover, effects of geometrical parameters, GPL distribution pattern, and amount of temperature change were also considered. In obtaining results of vibrational behavior, both analytical solution and deep neural network (DNN) methods were used. The most important outcome of the study can be encapsulated as follows:

- Utilizing MCS is vital in the investigation of nanostructure materials in both buckling and vibrational analysis since, on this scale, the material behavior is strongly size-dependent.

- The deep neural network can effectively predict the natural frequencies of the structures under various conditions.
- Increase in ΔT from 0 to 20K, the non-dimensional resonance frequency slightly decreases from 0.377 to 0.371 ($\sim$1.6%).
- Increase in l/R from 0 to 1/3 results in the non-dimensional resonance frequency increase from 0.153 to 0.178.
- Changing the pattern from GPL-A to GPL-O notably increases the resonance frequency. It is observed that GPL-A has the lowest resonance frequency while GPL-O has the highest resonance frequency.
- It is observed that at a certain values of temperature change, a spike in the relative natural frequency is seen in both MCS and classical theories excitation frequency increases with increase in the weight fraction of GPL.

References

Abualnour, M., Chikh, A., Hebali, H., Kaci, A., Tounsi, A., Bousahla Abdelmoumen, A. and Tounsi, A. (2019), "Thermomechanical analysis of antisymmetric laminated reinforced composite plates using a new four variable trigonometric refined plate theory", *Comput. Concrete*, **24**(6), 489-498. https://doi.org/10.12989/cac.2019.24.6.489.

Adamian, A., Safari, K.H., Sheikholeslami, M., Habibi, M., Al-Furjan, M. and Chen, G. (2020), "Critical temperature and frequency characteristics of GPLs-reinforced composite Doubly curved panel", *Appl. Sci.*, **10**(9), 3251. https://doi.org/10.3390/app10093251.

Affdl, J.H. and Kardos, J. (1976), "The Halpin-Tsai equations: a review", *Polymer Eng. Sci.*, **16**(5), 344-352. https://doi.org/10.1002/pen.760160512.

Al-Furjan, M., Alzahrani, B., Shan, L., Habibi, M. and Jung, D.W. (2020a), "Nonlinear forced vibrations of nanocomposite-reinforced viscoelastic thick annular system under hygrothermal environment", *Mech. Based Des. Struct.*, 1-27. https://doi.org/10.1080/15397734.2020.1824795.

Al-Furjan, M., Bolandi, S.Y., Habibi, M., Ebrahimi, F., Chen, G. and Safarpour, H. (2021), "Enhancing vibration performance of a spinning smart nanocomposite reinforced microstructure conveying fluid flow", *Eng. with Comput.*, 1-16. https://doi.org/10.1007/s00366-020-01255-w.

Al-Furjan, M., Bolandi, S.Y., Shan, L., Habibi, M. and Jung, D.W. (2020b), "On the vibrations of a high-speed rotating multi-hybrid nanocomposite reinforced cantilevered microdisk", *Mech. Based Des. Struct.*, 1-29. https://doi.org/10.1080/15397734.2020.1828098.

Al-Furjan, M., Dehini, R., Khorami, M., Habibi, M. and Won Jung, D. (2020c), "On the dynamics of the ultra-fast rotating cantilever orthotropic piezoelectric nanodisk based on nonlocal strain gradient theory", *Compos. Struct.*, 112990. https://doi.org/10.1016/j.compstruct.2020.112990.

Al-Furjan, M., Fereidouni, M., Habibi, M., Abd Ali, R., Ni, J. and Safarpour, M. (2020d), "Influence of in-plane loading on the vibrations of the fully symmetric mechanical systems via dynamic simulation and generalized differential quadrature framework", *Eng. with Comput.*, 1-23. https://doi.org/10.1007/s00366-020-01177-7.

Al-Furjan, M., Fereidouni, M., Sedghiyan, D., Habibi, M. and Won Jung, D. (2020e), "Three-dimensional frequency response of the CNT-Carbon-Fiber reinforced laminated circular/annular plates under initially stresses", *Compos. Struct.*, 113146. https://doi.org/10.1016/j.compstruct.2020.113146.

Al-Furjan, M., Habibi, M., Chen, G., Safarpour, H., Safarpour, M. and Tounsi, A. (2020f), "Chaotic oscillation of a multi-scale hybrid nano-composites reinforced disk under harmonic excitation via GDQM", *Compos. Struct.*, **252** 112737. https://doi.org/10.1016/j.compstruct.2020.112737.

Al-Furjan, M., Habibi, M., Chen, G., Safarpour, H., Safarpour, M. and Tounsi, A. (2020g), "Chaotic simulation of the multi-phase reinforced thermo-elastic disk using GDQM", *Eng. with Comput.*, 1-24. https://doi.org/10.1007/s00366-020-01144-2.

Al-Furjan, M., Habibi, M., Ebrahimi, F., Chen, G., Safarpour, M. and Safarpour, H. (2020h), "A coupled thermomechanics approach for frequency information of electrically composite microshell using heat-transfer continuum problem", *Eur. Phys. J. Plus.* **135**(10), 1-45. https://doi.org/10.1140/epjp/s13360-020-00764-3.

Al-Furjan, M., Habibi, M., Ebrahimi, F., Mohammadi, K. and Safarpour, H. (2020i), "Wave dispersion characteristics of high-speed-rotating laminated nanocomposite cylindrical shells based on four continuum mechanics theories", *Waves in Random and Complex Media*, 1-27. https://doi.org/10.1080/17455030.2020.1831099.

Al-Furjan, M., Habibi, M., Ghabussi, A., Safarpour, H., Safarpour, M. and Tounsi, A. (2020j), "Non-polynomial framework for stress and strain response of the FG-GPLRC disk using three-dimensional refined higher-order theory", *Eng. Struct.*, 111496. https://doi.org/10.1016/j.engstruct.2020.111496.

Al-Furjan, M., Habibi, M., Ni, J., Won Jung, D. and Tounsi, A. (2020k), "Frequency simulation of viscoelastic multi-phase reinforced fully symmetric systems", *Eng. with Comput.*, 1-17. https://doi.org/10.1007/s00366-020-01200-x.

Al-Furjan, M., Habibi, M. and Safarpour, H. (2020l), "Vibration control of a smart shell reinforced by graphene nanoplatelets", *Int. J. Appl. Mech.*, **12**(6), 2050066. https://doi.org/10.1142/S1758825120500660.

Al-Furjan, M., Habibi, M., Shan, L. and Tounsi, A. (2020n), "On the vibrations of the imperfect sandwich higher-order disk with a lactic core using generalize differential quadrature method", *Compos. Struct.*, 113150. https://doi.org/10.1016/j.compstruct.2020.113150.

Al-Furjan, M., Habibi, M., Won Jung, D., Chen, G., Safarpour, M. and Safarpour, H. (2020m), "Chaotic responses and nonlinear dynamics of the graphene nanoplatelets reinforced doubly-curved panel", *Eur. J. Mech.-A/Solids*, **85**, 104091. https://doi.org/10.1016/j.euromechsol.2020.104091.

Al-Furjan, M., Habibi, M., Won Jung, D., Sadeghi, S., Safarpour, H., Tounsi, A. and Chen, G. (2020p), "A computational framework for propagated waves in a sandwich doubly curved nanocomposite panel", *Eng. with Comput.*, 1-18. https://doi.org/10.1007/s00366-020-01130-8.

Al-Furjan, M., Habibi, M., Won Jung, D. and Safarpour, H. (2020q), "Vibrational characteristics of a higher-order laminated composite viscoelastic annular microplate via modified couple stress theory", *Compos. Struct.*, 113152. https://doi.org/10.1016/j.compstruct.2020.113152.

Al-Furjan, M., Habibi, M., Won Jung, D., Safarpour, H. and Safarpour, M. (2020r), "On the buckling of the polymer-CNT-fiber nanocomposite annular system under thermo-mechanical loads", *Mech. Based Des. Struct.*, 1-21. https://doi.org/10.1080/15397734.2020.1830106.

Al-Furjan, M., Moghadam, S.A., Dehini, R., Shan, L., Habibi, M. and Safarpour, H. (2020s), "Vibration control of a smart shell reinforced by graphene nanoplatelets under external load: Semi-

numerical and finite element modeling", *Thin-Wall. Struct.*, 107242. https://doi.org/10.1016/j.tws.2020.107242.

Al-Furjan, M., Mohammadgholiha, M., Alarifi, I.M., Habibi, M. and Safarpour, H. (2020t), "On the phase velocity simulation of the multi curved viscoelastic system via an exact solution framework", *Eng. with Computers.* 1-17. https://doi.org/10.1007/s00366-020-01152-2.

Al-Furjan, M., Oyarhossein, M.A., Habibi, M., Safarpour, H. and Jung, D.W. (2020u), "Frequency and critical angular velocity characteristics of rotary laminated cantilever microdisk via two-dimensional analysis", *Thin-Wall. Struct.*, **157** 107111. https://doi.org/10.1016/j.tws.2020.107111.

Al-Furjan, M., Oyarhossein, M.A., Habibi, M., Safarpour, H. and Jung, D.W. (2020v), "Wave propagation simulation in an electrically open shell reinforced with multi-phase nanocomposites", *Eng. with Comput.*, 1-17. https://doi.org/10.1007/s00366-020-01167-9.

Al-Furjan, M., Oyarhossein, M.A., Habibi, M., Safarpour, H., Jung, D.W. and Tounsi, A. (2020w), "On the wave propagation of the multi-scale hybrid nanocomposite doubly curved viscoelastic panel", *Compos. Struct.*, 112947. https://doi.org/10.1016/j.compstruct.2020.112947.

Al-Furjan, M., Safarpour, H., Habibi, M., Safarpour, M. and Tounsi, A. (2020x), "A comprehensive computational approach for nonlinear thermal instability of the electrically FG-GPLRC disk based on GDQ method", *Eng. with Comput.*, 1-18. https://doi.org/10.1007/s00366-020-01088-7.

Al-Furjan, M.S.H., Dehini, R., Paknahad, M., Habibi, M. and Safarpour, H. (2021b), "On the nonlinear dynamics of the multi-scale hybrid nanocomposite-reinforced annular plate under hygro-thermal environment", *Arch. Civil Mech. Eng.*, **21**(1), 4. https://doi.org/10.1007/s43452-020-00151-w.

Alimirzaei, S., Mohammadimehr, M. and Tounsi, A. (2019), "Nonlinear analysis of viscoelastic micro-composite beam with geometrical imperfection using FEM: MSGT electro-magneto-elastic bending, buckling and vibration solutions", *Struct. Eng. Mech.*, **71**(5), 485-502. https://doi.org/10.12989/sem.2019.71.5.485.

Alipour, M., Torabi, M.A., Sareban, M., Lashini, H., Sadeghi, E., Fazaeli, A., Habibi, M. and Hashemi, R. (2020), "Finite element and experimental method for analyzing the effects of martensite morphologies on the formability of DP steels", *Mech. Based Des. Struct.*, **48**(5), 525-541. https://doi.org/10.1080/15397734.2019.1633343.

Allam, O., Draiche, K., Bousahla Abdelmoumen, A., Bourada, F., Tounsi, A., Benrahou Kouider, H., Mahmoud, S.R., Adda Bedia, E.A. and Tounsi, A. (2020), "A generalized 4-unknown refined theory for bending and free vibration analysis of laminated composite and sandwich plates and shells", *Comput. Concrete*, **26**(2), 185-201. https://doi.org/10.12989/cac.2020.26.2.185.

Asghar, S., Naeem Muhammad, N., Hussain, M., Taj, M. and Tounsi, A. (2020), "Prediction and assessment of nonlocal natural frequencies of DWCNTs: Vibration analysis", *Comput. Concrete*, **25**(2), 133-144. https://doi.org/10.12989/cac.2020.25.2.133.

Bai, Y., Alzahrani, B., Baharom, S. and Habibi, M. (2020), "Semi-numerical simulation for vibrational responses of the viscoelastic imperfect annular system with honeycomb core under residual pressure", *Eng. with Comput.*, 1-26. https://doi.org/10.1007/s00366-020-01191-9.

Barooti, M.M., Safarpour, H. and Ghadiri, M. (2017), "Critical speed and free vibration analysis of spinning 3D single-walled carbon nanotubes resting on elastic foundations", *Eur. Phys. J. Plus.* **132**(1), 6. https://doi.org/10.1140/epjp/i2017-11275-5.

Belbachir, N., Bourada, M., Draiche, K., Tounsi, A., Bourada, F., Bousahla Abdelmoumen, A. and Mahmoud, S.R. (2020),

"Thermal flexural analysis of anti-symmetric cross-ply laminated plates using a four variable refined theory", *Smart Struct. Syst.*, **25**(4), 409-422. https://doi.org/10.12989/sss.2020.25.4.409.

Belbachir, N., Draich, K., Bousahla, A.A., Bourada, M., Tounsi, A. and Mohammadimehr, M. (2019), "Bending analysis of anti-symmetric cross-ply laminated plates under nonlinear thermal and mechanical loadings", *Steel Compos. Struct.*, **33**(1), 81-92. https://doi.org/10.12989/scs.2019.33.1.081.

Bourada, F., Bousahla Abdelmoumen, A., Tounsi, A., Bedia, E.A.A., Mahmoud, S.R., Benrahou Kouider, H. and Tounsi, A. (2020), "Stability and dynamic analyses of SW-CNT reinforced concrete beam resting on elastic-foundation", *Comput. Concrete*, **25**(6), 485-495. https://doi.org/10.12989/cac.2020.25.6.485.

Bousahla Abdelmoumen, A., Bourada, F., Mahmoud, S.R., Tounsi, A., Algarni, A., Bedia, E.A.A. and Tounsi, A. (2020a), "Buckling and dynamic behavior of the simply supported CNT-RC beams using an integral-first shear deformation theory", *Comput. Concrete*, **25**(2), 155-166. https://doi.org/10.12989/cac.2020.25.2.155.

Boussoula, A., Boucham, B., Bourada, M., Bourada, F., Tounsi, A., Bousahla Abdelmoumen, A. and Tounsi, A. (2020b), "A simple nth-order shear deformation theory for thermomechanical bending analysis of different configurations of FG sandwich plates", *Smart Struct. Syst.*, **25**(2), 197-218. https://doi.org/10.12989/sss.2020.25.2.197.

Challamel, N., Aydogdu, M. and Elishakoff, I. (2018), "Statics and dynamics of nanorods embedded in an elastic medium: Nonlocal elasticity and lattice formulations", *Eur. J. Mech.-A/Solids*, **67** 254-271. https://doi.org/10.1016/j.euromechsol.2017.09.009.

Cheshmeh, E., Karbon, M., Eyvazian, A., Jung, D.w., Habibi, M. and Safarpour, M. (2020), "Buckling and vibration analysis of FG-CNTRC plate subjected to thermo-mechanical load based on higher order shear deformation theory", *Mech. Based Des. Struct.*, 1-24. https://doi.org/10.1080/15397734.2020.1744005.

Dai, H. and Safarpour, H. (2021a), "Frequency and thermal buckling information of laminated composite doubly curved open nanoshell", *Adv. Nano Res.*, **10**(1), 1-14. https://doi.org/10.12989/anr.2021.10.1.001.

Dai, Z., Jiang, Z., Zhang, L. and Habibi, M. (2021b), "Frequency characteristics and sensitivity analysis of a size-dependent laminated nanoshell", *Adv. Nano Res.*, **10**(2), 175. https://doi.org/10.12989/anr.2021.10.2.175.

Dai, Z., Zhang, L., Bolandi, S.Y. and Habibi, M. (2021c), "On the vibrations of the non-polynomial viscoelastic composite open-type shell under residual stresses", *Compos. Struct.*, 113599. https://doi.org/10.1016/j.compstruct.2021.113599.

De Domenico, D. and Askes, H. (2018), "Stress gradient, strain gradient and inertia gradient beam theories for the simulation of flexural wave dispersion in carbon nanotubes", *Compos. Part B: Eng.*, **153**, 285-294. https://doi.org/10.1016/j.compositesb.2018.08.083.

De Domenico, D., Askes, H. and Aifantis, E.C. (2019), "Gradient elasticity and dispersive wave propagation: Model motivation and length scale identification procedures in concrete and composite laminates", *Int. J. Solids Struct.*, **158**, 176-190. https://doi.org/10.1016/j.ijsolstr.2018.09.007.

Ding, H., Bao, X., Jamili-Shirvan, Z., Jin, J., Deng, L., Yao, K., Gong, P. and Wang, X. (2021), "Enhancing strength-ductility synergy in an ex situ Zr-based metallic glass composite via nanocrystal formation within high-entropy alloy particles", *Mater. Design*, **210**, 110108. https://doi.org/10.1016/j.matdes.2021.110108.

Draiche, K., Bousahla Abdelmoumen, A., Tounsi, A., Alwabli Afaf, S., Tounsi, A. and Mahmoud, S.R. (2019), "Static analysis of laminated reinforced composite plates using a simple first-order shear deformation theory", *Comput. Concrete.* **24**(4), 369-378. https://doi.org/10.12989/cac.2019.24.4.369.

Ebrahimi, F., Habibi, M. and Safarpour, H. (2019a), "On modeling of wave propagation in a thermally affected GNP-reinforced imperfect nanocomposite shell", *Eng. with Comput.*, **35**(4), 1375-1389. https://doi.org/10.1007/s00366-018-0669-4

Ebrahimi, F., Hajilak, Z.E., Habibi, M. and Safarpour, H. (2019b), "Buckling and vibration characteristics of a carbon nanotube-reinforced spinning cantilever cylindrical 3D shell conveying viscous fluid flow and carrying spring-mass systems under various temperature distributions", *Proceedings of the Institution of Mechanical Engineers, Part C: Journal of Mechanical Engineering Science.* **233**(13), 4590-4605. https://doi.org/10.1177/0954406219832323.

Ebrahimi, F., Hashemabadi, D., Habibi, M. and Safarpour, H. (2020a), "Thermal buckling and forced vibration characteristics of a porous GNP reinforced nanocomposite cylindrical shell", *Microsystem Technologies*, **26**(2), 461-473. https://doi.org/10.1007/s00542-019-04542-9.

Ebrahimi, F., Mohammadi, K., Barouti, M.M. and Habibi, M. (2019c), "Wave propagation analysis of a spinning porous graphene nanoplatelet-reinforced nanoshell", *Waves in Random and Complex Media*, 1-27. https://doi.org/10.1080/17455030.2019.1694729.

Ebrahimi, F. and Safarpour, H. (2018), "Vibration analysis of inhomogeneous nonlocal beams via a modified couple stress theory incorporating surface effects", *Wind Struct.*, **27**(6), 431-438. https://doi.org/10.12989/was.2018.27.6.431.

Ebrahimi, F., Supeni, E.E.B., Habibi, M. and Safarpour, H. (2020b), "Frequency characteristics of a GPL-reinforced composite microdisk coupled with a piezoelectric layer", *Eur. Phys. J. Plus*, **135**(2), 144. https://doi.org/10.1140/epjp/s13360-020-00217-x.

Esmailpoor Hajilak, Z., Pourghader, J., Hashemabadi, D., Sharifi Bagh, F., Habibi, M. and Safarpour, H. (2019), "Multilayer GPLRC composite cylindrical nanoshell using modified strain gradient theory", *Mech. Based Des. Struct.*, **47**(5), 521-545. https://doi.org/10.1080/15397734.2019.1566743.

Ghabussi, A., Ashrafi, N., Shavalipour, A., Hosseinpour, A., Habibi, M., Moayedi, H., Babaei, B. and Safarpour, H. (2019), "Free vibration analysis of an electro-elastic GPLRC cylindrical shell surrounded by viscoelastic foundation using modified length-couple stress parameter", *Mech. Based Des. Struct.*, 1-25. https://doi.org/10.1080/15397734.2019.1705166.

Ghabussi, A., Habibi, M., NoormohammadiArani, O., Shavalipour, A., Moayedi, H. and Safarpour, H. (2020), "Frequency characteristics of a viscoelastic graphene nanoplatelet–reinforced composite circular microplate", *J. Vib. Control*, 1077546320923930. https://doi.org/10.1177/1077546320923930.

Ghazanfari, A., Soleimani, S.S., Keshavarzzadeh, M., Habibi, M., Assempuor, A. and Hashemi, R. (2020), "Prediction of FLD for sheet metal by considering through-thickness shear stresses", *Mech. Based Des. Struct.*, **48**(6), 755-772. https://doi.org/10.1080/15397734.2019.1662310.

Guo, J., Baharvand, A., Tazeddinova, D., Habibi, M., Safarpour, H., Roco-Videla, A. and Selmi, A. (2021a), "An intelligent computer method for vibration responses of the spinning multi-layer symmetric nanosystem using multi-physics modeling", *Eng. with Comput.*, 1-22. https://doi.org/10.1007/s00366-021-01433-4.

Guo, Y., Mi, H. and Habibi, M. (2021b), "Electromechanical energy absorption, resonance frequency, and low-velocity impact analysis of the piezoelectric doubly curved system",

Mech. Syst. Signal Pr., **157**, 107723. https://doi.org/10.1016/j.ymssp.2021.107723.

Habibi, M., Darabi, R., Sa, J.C.D. and Reis, A. (2021c), "An innovation in finite element simulation via crystal plasticity assessment of grain morphology effect on sheet metal formability", *Proceedings of the Institution of Mechanical Engineers, Part L: Journal of Materials: Design and Applications.* **235**(8), 1937-1951. https://doi.org/10.1177/14644207211024686.

Habibi, M., Ghazanfari, A., Assempour, A., Naghdabadi, R. and Hashemi, R. (2017), "Determination of forming limit diagram using two modified finite element models", *Mech Eng.*, **48**(4), 141-144. https://doi.org/10.22060/MEJ.2016.664.

Habibi, M., Hashemabadi, D. and Safarpour, H. (2019), "Vibration analysis of a high-speed rotating GPLRC nanostructure coupled with a piezoelectric actuator", *Eur. Phys. J. Plus*, **134**(6), 307. https://doi.org/10.1140/epjp/i2019-12742-7.

Habibi, M., Hashemi, R., Ghazanfari, A., Naghdabadi, R. and Assempour, A. (2018), "Forming limit diagrams by including the M–K model in finite element simulation considering the effect of bending", *Proceedings of the Institution of Mechanical Engineers, Part L: Journal of Materials: Design and Applications.* **232**(8), 625-636. https://doi.org/10.1177/1464420716642258.

Habibi, M., Hashemi, R., Sadeghi, E., Fazaeli, A., Ghazanfari, A. and Lashini, H. (2016), "Enhancing the mechanical properties and formability of low carbon steel with dual-phase microstructures", *J. Mater. Eng. Perform.*, **25**(2), 382-389. https://doi.org/10.1007/s11665-016-1882-1.

Habibi, M., Hashemi, R., Tafti, M.F. and Assempour, A. (2018), "Experimental investigation of mechanical properties, formability and forming limit diagrams for tailor-welded blanks produced by friction stir welding", *J. Manuf. Processes*, **31** 310-323. https://doi.org/10.1016/j.jmapro.2017.11.009.

Habibi, M., Mohammadgholiha, M. and Safarpour, H. (2019a), "Wave propagation characteristics of the electrically GNP-reinforced nanocomposite cylindrical shell", *J. Brazilian Soc. Mech. Sci. Eng.*, **41**(5), 221. https://doi.org/10.1007/s40430-019-1715-x.

Habibi, M., Mohammadi, A., Safarpour, H. and Ghadiri, M. (2019b), "Effect of porosity on buckling and vibrational characteristics of the imperfect GPLRC composite nanoshell", *Mech. Based Des. Struct.*, 1-30. https://doi.org/10.1080/15397734.2019.1701490.

Habibi, M., Mohammadi, A., Safarpour, H., Shavalipour, A. and Ghadiri, M. (2019c), "Wave propagation analysis of the laminated cylindrical nanoshell coupled with a piezoelectric actuator", *Mech. Based Des. Struct.*, 1-19. https://doi.org/10.1080/15397734.2019.1697932.

Habibi, M., Safarpour, M. and Safarpour, H. (2020), "Vibrational characteristics of a FG-GPLRC viscoelastic thick annular plate using fourth-order Runge-Kutta and GDQ methods", *Mech. Based Des. Struct.*, 1-22. https://doi.org/10.1080/15397734.2020.1779086.

Habibi, M., Taghdir, A. and Safarpour, H. (2019d), "Stability analysis of an electrically cylindrical nanoshell reinforced with graphene nanoplatelets", *Compos. Part B: Eng.*, **175**, 107125. https://doi.org/10.1016/j.compositesb.2019.107125.

Hashemi, H.R., Alizadeh, A.A., Oyarhossein, M.A., Shavalipour, A., Makkiabadi, M. and Habibi, M. (2019), "Influence of imperfection on amplitude and resonance frequency of a reinforcement compositionally graded nanostructure", *Waves in Random and Complex Media*, 1-27. https://doi.org/10.1080/17455030.2019.1662968.

He, X., Ding, J., Habibi, M., Safarpour, H. and Safarpour, M. (2021), "Non-polynomial framework for bending responses of the multi-scale hybrid laminated nanocomposite reinforced

circular/annular plate", *Thin-Wall. Struct.*, **166**, 108019. https://doi.org/10.1016/j.tws.2021.108019.

Hou, F., Wu, S., Moradi, Z. and Shafiei, N. (2021), "The computational modeling for the static analysis of axially functionally graded micro-cylindrical imperfect beam applying the computer simulation", *Eng. with Comput.*, 1-19. https://doi.org/10.1080/17455030.2019.1662968.

Huang, X., Hao, H., Oslub, K., Habibi, M. and Tounsi, A. (2021a), "Dynamic stability/instability simulation of the rotary size-dependent functionally graded microsystem", *Eng. with Comput.*, 1-17. https://doi.org/10.1007/s00366-021-01399-3.

Huang, X., Zhang, Y., Moradi, Z. and Shafiei, N. (2021b), "Computer simulation via a couple of homotopy perturbation methods and the generalized differential quadrature method for nonlinear vibration of functionally graded non-uniform micro-tube", *Eng. with Comput.*, 1-18. https://doi.org/10.1007/s00366-021-01395-7.

Huang, X., Zhu, Y., Vafaei, P., Moradi, Z. and Davoudi, M. (2021c), "An iterative simulation algorithm for large oscillation of the applicable 2D-electrical system on a complex nonlinear substrate", *Eng. with Comput.*, https://doi.org/10.1007/s00366-021-01320-y.

Huo, J., Zhang, G., Ghabussi, A. and Habibi, M. (2021), "Bending analysis of FG-GPLRC axisymmetric circular/annular sector plates by considering elastic foundation and horizontal friction force using 3D-poroelasticity theory", *Compos. Struct.*, 114438. https://doi.org/10.1016/j.compstruct.2021.114438.

Hussain, M., Naeem Muhammad, N., Khan Muhammad, S. and Tounsi, A. (2020), "Computer-aided approach for modelling of FG cylindrical shell sandwich with ring supports", *Comput. Concrete*, **25**(5), 411-425. https://doi.org/10.12989/cac.2020.25.5.411.

Hussain, M., Naeem Muhammad, N., Tounsi, A. and Taj, M. (2019), "Nonlocal effect on the vibration of armchair and zigzag SWCNTs with bending rigidity", *Adv. Nano Res.*, **7**(6), 431-442. https://doi.org/10.12989/anr.2019.7.6.431.

Jermsittiparsert, K., Ghabussi, A., Forooghi, A., Shavalipour, A., Habibi, M., Won Jung, D. and Safa, M. (2020), "Critical voltage, thermal buckling and frequency characteristics of a thermally affected GPL reinforced composite microdisk covered with piezoelectric actuator", *Mech. Based Des. Struct.*, 1-23. ttps://doi.org/10.1080/15397734.2020.1748052.

Jiao, J., Ghoreishi, S.-m., Moradi, Z. and Oslub, K. (2021), "Coupled particle swarm optimization method with genetic algorithm for the static–dynamic performance of the magneto-electro-elastic nanosystem", *Eng. with Comput.*, https://doi.org/10.1007/s00366-021-01391-x

Karami, B., Janghorban, M. and Tounsi, A. (2019), "On pre-stressed functionally graded anisotropic nanoshell in magnetic field", *J. Braz. Soc. Mech. Sci. Eng.*, **41**(11), 495. https://doi.org/10.1007/s40430-019-1996-0.

Khorasani, M., Eyvazian, A., Karbon, M., Tounsi, A., Lampani, L. and Sebaey Tamer, A. (2020), "Magneto-electro-elastic vibration analysis of modified couple stress-based three-layered micro rectangular plates exposed to multi-physical fields considering the flexoelectricity effects", *Smart Struct. Syst.*, **26**(3), 331-343. https://doi.org/10.12989/SSS.2020.26.3.331.

Li, Y., Li, S., Guo, K., Fang, X. and Habibi, M. (2020), "On the modeling of bending responses of graphene-reinforced higher order annular plate via two-dimensional continuum mechanics approach", *Eng. with Comput.*, 1-22. https://doi.org/10.1080/15397734.2020.1779086.

Liu, H., Shen, S., Oslub, K., Habibi, M. and Safarpour, H. (2021a), "Amplitude motion and frequency simulation of a composite viscoelastic microsystem within modified couple stress elasticity", *Eng. with Comput.*, 1-15. https://doi.org/10.1007/s00366-021-01316-8.

Liu, H., Zhao, Y., Pishbin, M., Habibi, M., Bashir, M. and Issakhov, A. (2021b), "A comprehensive mathematical simulation of the composite size-dependent rotary 3D microsystem via two-dimensional generalized differential quadrature method", *Eng. with Comput.*, 1-16. https://doi.org/10.1007/s00366-021-01419-2.

Liu, Y., Wang, W., He, T., Moradi, Z. and Larco Benítez, M.A. (2021c), "On the modelling of the vibration behaviors via discrete singular convolution method for a high-order sector annular system", *Eng. with Comput.*, 1-23. https://doi.org/10.1080/15397734.2020.1779086.

Liu, Z., Su, S., Xi, D. and Habibi, M. (2020a), "Vibrational responses of a MHC viscoelastic thick annular plate in thermal environment using GDQ method", *Mech. Based Des. Struct.*, 1-26. https://doi.org/10.1080/15397734.2020.1784201.

Liu, Z., Wu, X., Yu, M. and Habibi, M. (2020b), "Large-amplitude dynamical behavior of multilayer graphene platelets reinforced nanocomposite annular plate under thermo-mechanical loadings", *Mech. Based Des. Struct.*, 1-25. https://doi.org/10.1080/15397734.2020.1815544.

Lori, E.S., Ebrahimi, F., Supeni, E.E.B., Habibi, M. and Safarpour, H. (2020), "The critical voltage of a GPL-reinforced composite microdisk covered with piezoelectric layer", *Eng. with Comput.*, 1-20. https://doi.org/10.1007/s00366-020-01004-z.

Ma, L., Liu, X. and Moradi, Z. (2021), "On the chaotic behavior of graphene-reinforced annular systems under harmonic excitation", *Eng. with Comput.*, 1-25. https://doi.org/10.1007/s00366-020-01210-9.

Matouk, H., Bousahla Abdelmoumen, A., Heireche, H., Bourada, F., Bedia, E.A.A., Tounsi, A., Mahmoud, S.R., Tounsi, A. and Benrahou, K.H. (2020), "Investigation on hygro-thermal vibration of P-FG and symmetric S-FG nanobeam using integral Timoshenko beam theory", *Adv. Nano Res.*, **8**(4), 293-305. https://doi.org/10.12989/anr.2020.8.4.293.

Menasria, A., Kaci, A., Bousahla, A.A., Bourada, F., Tounsi, A., Benrahou, K.H., Tounsi, A., Adda Bedia, E. and Mahmoud, S. (2020), "A four-unknown refined plate theory for dynamic analysis of FG-sandwich plates under various boundary conditions", *Steel Compos. Struct.*, **36**(3), 355-367. https://doi.org/10.12989/scs.2020.36.3.355.

Meng, Q., Lai, X., Yan, Z., Su, C.Y. and Wu, M. (2021), "Motion planning and adaptive neural tracking control of an uncertain two-link rigid-flexible manipulator with vibration amplitude constraint", *IEEE T. Neural Networ.*, 10.1109/TNNLS.2021.3054611

Moayedi, H., Aliakbarlou, H., Jebeli, M., Noormohammadiarani, O., Habibi, M., Safarpour, H. and Foong, L. (2020a), "Thermal buckling responses of a graphene reinforced composite micropanel structure", *Int. J. Appl. Mech.*, **12**(1), 2050010. https://doi.org/10.1142/S1758825120500106.

Moayedi, H., Darabi, R., Ghabussi, A., Habibi, M. and Foong, L.K. (2020b), "Weld orientation effects on the formability of tailor welded thin steel sheets", *Thin-Wall. Struct.*, **149**, 106669. https://doi.org/10.1016/j.tws.2020.106669.

Moayedi, H., Ebrahimi, F., Habibi, M., Safarpour, H. and Foong, L.K. (2020c), "Application of nonlocal strain–stress gradient theory and GDQEM for thermo-vibration responses of a laminated composite nanoshell", *Eng. with Comput.*, 1-16. https://doi.org/10.1007/s00366-020-01002-1.

Moayedi, H., Habibi, M., Safarpour, H., Safarpour, M. and Foong, L. (2019), "Buckling and frequency responses of a graphene nanoplatelet reinforced composite microdisk", *Int. J. Appl. Mech.*, **11**(10), 1950102. https://doi.org/10.1142/S1758825119501023.

Mohammadgholiha, M., Shokrgozar, A., Habibi, M. and Safarpour, H. (2019), "Buckling and frequency analysis of the nonlocal strain–stress gradient shell reinforced with graphene

nanoplatelets", *J. Vib. Control*, **25**(19-20), 2627-2640. https://doi.org/10.1177/1077546319863251.

Mohammadi, A., Lashini, H., Habibi, M. and Safarpour, H. (2019), "Influence of viscoelastic foundation on dynamic behaviour of the double walled cylindrical inhomogeneous micro shell using MCST and with the aid of GDQM", *J. Solid Mech.*, **11**(2), 440-453. 10.22034/JSM.2019.665264.

Moradi, Z., Davoudi, M., Ebrahimi, F. and Ehyaei, A.F. (2021), "Intelligent wave dispersion control of an inhomogeneous micro-shell using a proportional-derivative smart controller", *Waves in Random and Complex Media*, 1-24. https://doi.org/10.1016/j.tws.2020.106669.

Najaafi, N., Jamali, M., Habibi, M., Sadeghi, S., Jung, D.W. and Nabipour, N. (2020), "Dynamic instability responses of the substructure living biological cells in the cytoplasm environment using stress-strain size-dependent theory", *J. Biomol. Struct. Dyn.*, 1-12. https://doi.org/10.1080/07391102.2020.1751297.

Ni, T., Liu, D., Xu, Q., Huang, Z., Liang, H. and Yan, A. (2020a), "Architecture of cobweb-based redundant TSV for clustered faults", *IEEE T. Very Large Scale Integration (VLSI) Systems*, **28**(7), 1736-1739. 10.1109/TVLSI.2020.2995094

Ni, T., Yang, Z., Chang, H., Zhang, X., Lu, L., Yan, A., Huang, Z. and Wen, X. (2020b), "A novel TDMA-based fault tolerance technique for the TSVs in 3D-ICs using honeycomb topology", *IEEE T. Emerging Topics Comput.*, **9**(2), 724-734. https://doi.org/10.1109/TETC.2020.2969237.

Oyarhossein, M.A., Alizadeh, A.a., Habibi, M., Makkiabadi, M., Daman, M., Safarpour, H. and Jung, D.W. (2020), "Dynamic response of the nonlocal strain-stress gradient in laminated polymer composites microtubes", *Scientific Reports*, **10**(1), 1-19. https://doi.org/10.1038/s41598-020-61855-w.

Pandit, S.G., Puttananjaiah, M.H., Peddha, M.S. and Dhale, M.A. (2020), "Safety efficacy and chemical profiling of water-soluble Talaromyces purpureogenus CFRM02 pigment", *Food Chemistry*, **310**, 125869. https://doi.org/10.1016/j.foodchem.2019.125869.

Peng, D., Chen, S., Darabi, R., Ghabussi, A. and Habibi, M. (2021), "Prediction of the bending and out-of-plane loading effects on formability response of the steel sheets", *Arch. Civil Mech. Eng.*, **21**(2), 74. https://doi.org/10.1007/s43452-021-00227-1.

Pourjabari, A., Hajilak, Z.E., Mohammadi, A., Habibi, M. and Safarpour, H. (2019), "Effect of porosity on free and forced vibration characteristics of the GPL reinforcement composite nanostructures", *Comput. Math. Appl.*, **77**(10), 2608-2626.

Refrafi, S., Bousahla Abdelmoumen, A., Bouhadra, A., Menasria, A., Bourada, F., Tounsi, A., Bedia, E.A.A., Mahmoud, S.R., Benrahou Kouider, H. and Tounsi, A. (2020), "Effects of hygro-thermo-mechanical conditions on the buckling of FG sandwich plates resting on elastic foundations", *Comput. Concrete*, **25**(4), 311-325. https://doi.org/10.12989/cac.2020.25.4.311.

SafarPour, H. and Ghadiri, M. (2017a), "Critical rotational speed, critical velocity of fluid flow and free vibration analysis of a spinning SWCNT conveying viscous fluid", *Microfluidics and Nanofluidics*, **21**(2), 22. https://doi.org/10.1007/s10404-017-1858-y

Safarpour, H., Ghanizadeh, S.A. and Habibi, M. (2018), "Wave propagation characteristics of a cylindrical laminated composite nanoshell in thermal environment based on the nonlocal strain gradient theory", *Eur. Phys. J. Plus*, **133**(12), 532.

Safarpour, H., Hajilak, Z.E. and Habibi, M. (2019), "A size-dependent exact theory for thermal buckling, free and forced vibration analysis of temperature dependent FG multilayer GPLRC composite nanostructures restring on elastic foundation", *Int. J. Mech. Mater. Design*, **15**(3), 569-583.

SafarPour, H., Hosseini, M. and Ghadiri, M. (2017b), "Influence of three-parameter viscoelastic medium on vibration behavior of a cylindrical nonhomogeneous microshell in thermal environment: An exact solution", *J. Therm. Stresses*, **40**(11), 1353-1367. https://doi.org/10.1080/01495739.2017.1350827.

SafarPour, H., Mohammadi, K., Ghadiri, M. and Rajabpour, A. (2017c), "Influence of various temperature distributions on critical speed and vibrational characteristics of rotating cylindrical microshells with modified lengthscale parameter", *Eur. Phys. J. Plus*, **132**(6), 1-19. https://doi.org/10.1140/epjp/i2017-11551-4.

Safarpour, H., Pourghader, J. and Habibi, M. (2019), "Influence of spring-mass systems on frequency behavior and critical voltage of a high-speed rotating cantilever cylindrical three-dimensional shell coupled with piezoelectric actuator", *J. Vib. Control*, **25**(9), 1543-1557. https://doi.org/10.1177/1077546319828465.

Safarpour, M., Ebrahimi, F., Habibi, M. and Safarpour, H. (2020), "On the nonlinear dynamics of a multi-scale hybrid nanocomposite disk", *Eng. with Comput.*, 1-20. https://doi.org/10.1007/s00366-020-00949-5.

Safarpour, M., Ghabussi, A., Ebrahimi, F., Habibi, M. and Safarpour, H. (2020), "Frequency characteristics of FG-GPLRC viscoelastic thick annular plate with the aid of GDQM", *Thin-Wall. Struct.*, **150**, 106683. https://doi.org/10.1016/j.tws.2020.106683.

Shahsiah, R. and Eslami, M. (2003), "Thermal buckling of functionally graded cylindrical shell", *J. Therm. Stresses*, **26**(3), 277-294. https://doi.org/10.1080/713855892.

Shao, Y., Zhao, Y., Gao, J. and Habibi, M. (2021), "Energy absorption of the strengthened viscoelastic multi-curved composite panel under friction force", *Arch. Civil Mech. Eng.*, **21**(4), 1-29.

Shariati, A., Ghabussi, A., Habibi, M., Safarpour, H., Safarpour, M., Tounsi, A. and Safa, M. (2020a), "Extremely large oscillation and nonlinear frequency of a multi-scale hybrid disk resting on nonlinear elastic foundation", *Thin-Wall. Struct.*, **154**, 106840. https://doi.org/10.1016/j.tws.2020.106840.

Shariati, A., Habibi, M., Tounsi, A., Safarpour, H. and Safa, M. (2020b), "Application of exact continuum size-dependent theory for stability and frequency analysis of a curved cantilevered microtubule by considering viscoelastic properties", *Eng. with Comput.*, 1-20. https://doi.org/10.1007/s00366-020-01024-9.

Shariati, A., Mohammad-Sedighi, H., Żur, K.K., Habibi, M. and Safa, M. (2020c), "On the vibrations and stability of moving viscoelastic axially functionally graded nanobeams", *Materials*, **13**(7), 1707. https://doi.org/10.3390/ma13071707.

Shariati, A., Mohammad-Sedighi, H., Żur, K.K., Habibi, M. and Safa, M. (2020d), "Stability and dynamics of viscoelastic moving rayleigh beams with an asymmetrical distribution of material parameters", *Symmetry*, **12**(4), 586. https://doi.org/10.3390/sym12040586.

Shi, G., Araby, S., Gibson, C.T., Meng, Q., Zhu, S. and Ma, J. (2018), "Graphene platelets and their polymer composites: fabrication, structure, properties, and applications", *Adv. Funct. Mater.*, **28**(19), 1706705. https://doi.org/10.1002/adfm.201706705.

Shi, M., Wang, F., Lan, P., Zhang, Y., Zhang, M., Yan, Y. and Liu, Y. (2021), "Effect of ultrasonic intensity on structure and properties of wheat starch-monoglyceride complex and its influence on quality of norther-style Chinese steamed bread", *LWT*, **138**, 110677. https://doi.org/10.1016/j.lwt.2020.110677.

Shi, X., Li, J. and Habibi, M. (2020), "On the statics and dynamics of an electro-thermo-mechanically porous GPLRC nanoshell conveying fluid flow", *Mech. Based Des. Struct.*, 1-37. https://doi.org/10.1080/15397734.2020.1772088

Shokrgozar, A., Ghabussi, A., Ebrahimi, F., Habibi, M. and Safarpour, H. (2020a), "Viscoelastic dynamics and static responses of a graphene nanoplatelets-reinforced composite cylindrical microshell", *Mech. Based Des. Struct.*, 1-28. https://doi.org/10.1080/15397734.2020.1719509.

Shokrgozar, A., Safarpour, H. and Habibi, M. (2020b), "Influence of system parameters on buckling and frequency analysis of a spinning cantilever cylindrical 3D shell coupled with piezoelectric actuator", *Proceedings of the Institution of Mechanical Engineers, Part C: Journal of Mechanical Engineering Science*, **234**(2), 512-529. https://doi.org/10.1177/0954406219883312.

Tadi Beni, Y., Mehralian, F. and Zeighampour, H. (2016), "The modified couple stress functionally graded cylindrical thin shell formulation", *Mech. Adv. Mater. Struct.*, **23**(7), 791-801. https://doi.org/10.1080/15376494.2015.1029167.

Tlidji, Y., Zidour, M., Draiche, K., Safa, A., Bourada, M., Tounsi, A., Bousahla, A.A. and Mahmoud, S. (2019), "Vibration analysis of different material distributions of functionally graded microbeam", *Struct. Eng. Mech.*, **69**(6), 637-649. https://doi.org/10.12989/sem.2019.69.6.637.

Tounsi, A., Al-Dulaijan, S., Al-Osta, M.A., Chikh, A., Al-Zahrani, M., Sharif, A. and Tounsi, A. (2020), "A four variable trigonometric integral plate theory for hygro-thermo-mechanical bending analysis of AFG ceramic-metal plates resting on a two-parameter elastic foundation", *Steel Compos. Struct.*, **34**(4), 511-524. https://doi.org/10.12989/scs.2020.34.4.511.

Wang, H., Zhang, H., Dousti, R. and Safarpour, H. (2021), "Dynamic simulation of moderately thick annular system coupled with shape memory alloy and multi-phase nanocomposite face sheets", *Eng. with Comput.*, 1-24. https://doi.org/10.1007/s00366-020-01246-x.

Wang, Z., Yu, S., Xiao, Z. and Habibi, M. (2020), "Frequency and buckling responses of a high-speed rotating fiber metal laminated cantilevered microdisk", *Mech. Adv. Mater. Struct.*, 1-14.

Wu, H., Kitipornchai, S. and Yang, J. (2017), "Thermal buckling and postbuckling of functionally graded graphene nanocomposite plates", *Mater. Design*, **132**, 430-441. https://doi.org/10.1016/j.matdes.2017.07.025.

Wu, J. and Habibi, M. (2021), "Dynamic simulation of the ultra-fast-rotating sandwich cantilever disk via finite element and semi-numerical methods", *Eng. with Comput.*, 1-17. https://doi.org/10.1007/s00366-021-01396-6.

Xu, W., Pan, G., Moradi, Z. and Shafiei, N. (2021), "Nonlinear forced vibration analysis of functionally graded non-uniform cylindrical microbeams applying the semi-analytical solution", *Compos. Struct.*, 114395. https://doi.org/10.1016/j.compstruct.2021.114395.

Yegnanarayana, B. (2009), *Artificial neural networks*, PHI Learning Pvt. Ltd.

Yu, X., Maalla, A. and Moradi, Z. (2022), "Electroelastic high-order computational continuum strategy for critical voltage and frequency of piezoelectric NEMS via modified multi-physical couple stress theory", *Mech. Syst. Signal Pr.*, **165**, 108373. https://doi.org/10.1016/j.ymssp.2021.108373.

Yu, X., Sun, Y., Zhao, D. and Wu, S. (2021), "A revised contact stiffness model of rough curved surfaces based on the length scale", *Tribology Int.*, **164**, 107206. https://doi.org/10.1016/j.triboint.2021.107206.

Zare, R., Najaafi, N., Habibi, M., Ebrahimi, F. and Safarpour, H. (2020), "Influence of imperfection on the smart control frequency characteristics of a cylindrical sensor-actuator GPLRC cylindrical shell using a proportional-derivative smart controller", *Smart Struct. Syst.*, **26**(4), 469-480. https://doi.org/10.12989/sss.2020.26.4.469.

Zeiler, M.D. (2012), "Adadelta: an adaptive learning rate method", *arXiv preprint arXiv:1212.5701*.

Zhang, B., Li, H., Kong, L., Shen, H. and Zhang, X. (2020), "Coupling effects of surface energy, strain gradient, and inertia gradient on the vibration behavior of small-scale beams", *Int. J. Mech. Sci.*, **184**, 105834. https://doi.org/10.1016/j.ijmecsci.2020.105834.

Zhang, L., Chen, Z., Habibi, M., Ghabussi, A. and Alyousef, R. (2021), "Low-velocity impact, resonance, and frequency responses of FG-GPLRC viscoelastic doubly curved panel", *Compos. Struct.*, **269**, 114000. https://doi.org/10.1016/j.compstruct.2021.114000.

Zhang, W., Liu, Z., Liang, Z., Oslub, K. and Safarpour, H. (2021), "A comprehensive computer simulation of the size-dependent sector or complete microsystem via two-dimensional generalized differential quadrature method", *Eng. with Comput.*, 1-17. https://doi.org/10.1007/s00366-021-01440-5.

Zhang, X., Shamsodin, M., Wang, H., NoormohammadiArani, O., Khan, A.M., Habibi, M. and Al-Furjan, M. (2020), "Dynamic information of the time-dependent tobullian biomolecular structure using a high-accuracy size-dependent theory", *J. Biomol. Struct. Dyn.*, 1-16. https://doi.org/10.1080/07391102.2020.1760939.

Zhang, X., Tang, Y., Zhang, F. and Lee, C.S. (2016), "A novel aluminum–graphite dual-ion battery", *Adv. Energy Mater.*, **6**(11), 1502588. https://doi.org/10.1002/aenm.201502588.

Zhang, Y., Wang, Z., Tazeddinova, D., Ebrahimi, F., Habibi, M. and Safarpour, H. (2021), "Enhancing active vibration control performances in a smart rotary sandwich thick nanostructure conveying viscous fluid flow by a PD controller", *Waves in Random and Complex Media*, 1-24. https://doi.org/10.1080/17455030.2021.1948627.

Zhao, H., Wang, L., Issakhov, A. and Safarpour, H. (2021), "Poroelasticity framework for stress/strain responses of the multi-phase circular/annular systems resting on various types of elastic foundations", *Eur. Phys. J. Plus*, **136**(8), 1-44. https://doi.org/10.1140/epjp/s13360-021-01761-w.

Zhao, Y., Moradi, Z., Davoudi, M. and Zhuang, J. (2021), "Bending and stress responses of the hybrid axisymmetric system via state-space method and 3D-elasticity theory", *Eng. with Comput.*, 1-23. https://doi.org/10.1007/s00366-020-01242-1.

Zhong, P.F., Lin, H.M., Wang, L.W., Mo, Z.Y., Meng, X.J., Tang, H.T. and Pan, Y.M. (2020), "Electrochemically enabled synthesis of sulfide imidazopyridines via a radical cyclization Cascade", *Green Chemistry*, https://doi.org/10.1039/D0GC02125C.

Zhou, C., Zhao, Y., Zhang, J., Fang, Y. and Habibi, M. (2020), "Vibrational characteristics of multi-phase nanocomposite reinforced circular/annular system", *Adv. Nano Res.*, **9**(4), 295-307. https://doi.org/10.12989/anr.2020.9.4.295.

Zine, A., Bousahla Abdelmoumen, A., Bourada, F., Benrahou Kouider, H., Tounsi, A., Adda Bedia, E.A., Mahmoud, S.R. and Tounsi, A. (2020), "Bending analysis of functionally graded porous plates via a refined shear deformation theory", *Comput. Concrete*, **26**(1), 63-74. https://doi.org/10.12989/cac.2020.26.1.063.

CC